

Multi-Agent Disk Inspection ^{*}

James Conley and Konstantinos Georgiou^{**}

Department of Mathematics, Toronto Metropolitan University, Toronto, ON, Canada
j1conley,konstantinos@torontomu.ca

Abstract. We consider n unit-speed mobile agents initially positioned at the center of a unit disk, tasked with inspecting all points on the disk's perimeter. A perimeter point is considered covered if an agent positioned outside the disk's interior has unobstructed visibility of it, treating the disk itself as an obstacle. For $n = 1$, this problem is referred to as the shoreline problem with a known distance and was originally proposed as a more tractable variant of Bellman's famous lost-in-the-forest problem [14]. Isbell [46] derived an optimal trajectory that minimizes the worst-case inspection time for that problem. For $n \geq 2$ agents, worst-case optimal trajectories were shown in [1,30].

Our contributions are threefold. First, and as a warm-up, we extend Isbell's findings by deriving worst-case optimal trajectories addressing the partial inspection of a section of the disk, hence deriving an alternative proof of optimality for inspecting the disk with $n \geq 2$ agents. Second, we analyze the average-case inspection time, assuming a uniform distribution of perimeter points (equivalent to randomized inspection algorithms). Using spatial discretization and Nonlinear Programming (NLP), we propose feasible solutions to the continuous problem and evaluate their effectiveness compared to NLP solutions. Third, we establish Pareto-optimal bounds for the multi-objective problem of jointly minimizing the worst-case and average-case inspection times.

Mobile Agents, Search, Disk, Shoreline Problem

^{*} This is the full version of the paper [24] with the same title, which was accepted and will be included in the proceedings of the 32nd International Colloquium on Structural Information and Communications Complexity (SIROCCO 2025), to be held on June 2–4, 2025, in Delphi, Greece.

^{**} Research supported in part by NSERC Discovery grant and by the Toronto Metropolitan University Faculty of Science Dean's Research Fund.

Table of Contents

Multi-Agent Disk Inspection	1
<i>James Conley and Konstantinos Georgiou</i>	
1 Introduction.....	3
1.1 Related Work.....	3
1.2 Roadmap.....	4
2 Inspection Problems and New Contributions.....	4
2.1 Formal Definition & Some Auxiliary Problems	4
2.2 Main Results Made Formal & Motivation.....	6
3 Optimal Worst Case Inspection for \mathcal{S}_n	8
3.1 Some Preliminary Observations	8
3.2 Solving \mathcal{S}_n Using the Partial Inspection Problem $\mathcal{P}(c)$	10
4 Average-Case Inspection Upper Bounds for \mathcal{S}_n	13
4.1 Discrete Inspection Algorithms for $\mathcal{A}(k, \theta, c)$ and $\mathcal{P}(c)$	13
4.2 Upper Bounds to the Average Case Inspection of $\mathcal{P}(c)$ and \mathcal{S}_n	17
5 Worst/Average Case Inspection Trade-offs to \mathcal{S}_1	20
5.1 Pareto Upper Bounds.....	20
References	24
A Omitted Proofs	27
A.1 Proofs Omitted from Section 3.2	27
B Omitted Figures	29
B.1 Figures Omitted from Section 4.2	29
B.2 Figures Omitted from Section 5	30

1 Introduction

In 1955, Bellman [14] posed a seminal question in search theory: given a random point P within a region R , what trajectory minimizes the expected time to reach the boundary, and what is the maximum time required? This question laid the groundwork for search theory, inspiring subsequent research into optimal trajectories under uncertainty. Bellman also proposed studying specific cases, such as when R represents the area between two parallel lines separated by a known distance or when R is a semi-infinite plane with a known distance to the boundary. This problem also appears in Bellman’s classic work on dynamic programming [15] (Problem 6, page 133), now recognized as the “lost-in-a-forest” problem. Over the decades, this question has inspired various modifications, with only a few specific cases fully resolved and many still open (see Section 1.1 for additional references). This question is a central reference in search theory [17] and has even appeared in the USSR Olympiad Problem Book [57]. Notably, the variant with two parallel lines is among the few examples that have been fully solved (see Problem 7, page 133, in [15]).

Bellman [14] introduced a notable variation of the problem as a simpler alternative to the lost-in-a-forest problem. This variation, solved by Isbell [46], is known as the *shoreline problem with known distance*. The problem seeks a minimum-length curve in \mathbb{R}^2 whose convex hull contains a disk of radius 1 centered at one endpoint. Alternatively, in modern mobile agent terms, it involves a unit-speed mobile agent tasked with finding a hidden infinite (shore)line at a known distance of 1, though its location is unknown. Isbell’s solution provides the agent’s optimal trajectory, minimizing the worst-case time to reach the shoreline.

The shoreline can also be interpreted as the visibility boundary for an agent tasked with inspecting (or patrolling) the perimeter of a unit disk, starting from its center. This application could represent inspecting the perimeter of a circular building for defects or intruders, where visibility of the exterior is possible only from outside the building. Specifically, a point on the disk is considered visible (inspected) if no convex combination of the agent’s position and the point lies within the disk’s interior, treating the disk as an obstacle to visibility. We refer to this task as the *1-agent inspection problem*, which Isbell resolved optimally by minimizing the worst-case inspection cost. Although originally posed as a theoretical question, Isbell’s shoreline problem laid the groundwork for modern applications in operations research, particularly in autonomous navigation and notably in navy operations.

To the best of our knowledge, we are the first to consider the *multi-agent* variant of this problem. Our work explores both *worst-case* and *average-case* (equivalent to considering randomized search trajectories for) inspection times for n agents, with a focus on the *partial inspection problem*, where an agent is tasked to inspect only an arc of some fixed length on the unit disk. This generalization allows us to develop solutions for the multi-agent case, optimizing both worst-case and average-case costs. Our approach involves discretizing the problem, constructing feasible trajectories through Nonlinear Programming solutions, and quantifying inspection costs across discrete and continuous settings, thus enabling us also to address the multi-objective optimization of minimizing both worst-case and average-case costs.

1.1 Related Work

The study of search problems began in the 1950s and 1960s [12,16] and has since become a distinct field within operations research and theoretical computer science. Foundational surveys and texts [2,3,4,27,38] document its development. Early research focused on single-agent line search [8,48], while advances in robotics spurred interest in multi-agent variants [25,53].

In search problems, agents aim to locate hidden targets within a domain. Linear search problems, such as the classic cow-path problem, are fundamental and have been extensively

studied for single [9] and multiple agents [21]. Recent work introduces variations minimizing weighted completion times [42] and adapts searches to complex domains such as rays [20], terrains [29], and graphs [5].

Two-dimensional search introduces added complexity, with early results for polygons [34] and disks [25], and expanded to include shapes like triangles, squares, ℓ_p disks, and regular polygons [10,28,39,41,40]. Multi-agent models in these contexts address coordination, speed [11], and fault tolerance [13,18,26]. The only related work addressing worst-case and average-case trade-offs in mobile agent search is in [22], examining single-agent search and evacuation in a unit disk.

The two-dimensional search problem most relevant to our work is Bellman’s shoreline problem [15], which was first solved optimally in the worst-case sense for a single agent by Isbell [46], with the target shoreline at a known distance from the agent’s starting point. Searching for a shoreline at a known distance with $n \geq 4$ agents was solved optimally in the worst-case sense in [1], while the cases of $n = 2, 3$ were treated in [30].

The more general lost-in-a-forest problem has been surveyed in [17,35]. Recent progress on the area include that for convex polygons in [43] and well as for general shapes using competitive analysis in [49]. Searching for a (shore)line without knowledge of its distance was introduced for a single robot in [8], with extensions for $n \geq 2$ robots explored in [6,7,9,47]. For $n = 1$, a logarithmic spiral achieves the best known competitive ratio of 13.81 [8,36], with lower bounds of 6.3972 unconditionally [7] and 12.5385 for cyclic trajectories [51]. For multiple robots, a double logarithmic spiral yields a competitive ratio of 5.2644 for $n = 2$ [7], and for $n \geq 3$, robots moving along rays achieve competitive ratio at most $1/\cos(\pi/n)$ [7], with matching lower bounds provided for $n \geq 4$ and $n = 3$ in [1] and [30], respectively. Variants where partial information is available yield varying competitive ratios based on distance, slope, or orientation knowledge [8,46,44,45,47].

Beyond shoreline search, strategies have been developed for circles [45] and other planar regions. Langetepe [50] proved that the spiral search is optimal for single-agent point search in two dimensions, while multi-agent and grid-based searches with memory constraints have been examined in [32,33,37,52]. Recent studies address point search in planar and geometric terrains [19,54] and explore trade-offs between search cost and information [56,55].

1.2 Roadmap

Section 2 presents the necessary preliminaries and result statements. Specifically, Section 2.1 formally introduces the problems studied and defines the notation, while Section 2.2 summarizes all results with appropriate quantification. The worst-case analysis begins in Section 3, with key inspection-related observations made and proved in Section 3.1. Section 3.2 then addresses the partial inspection problem, followed by the n -agent inspection problem for the worst case. The average-case problem is examined in Section 4. Specifically, Section 4.1 presents a discretized algorithm for the problem and quantifies its performance. This foundation allows us to address the partial continuous average inspection problem in Section 4.2. Finally, Section 5 explores the multi-objective problem.

2 Inspection Problems and New Contributions

2.1 Formal Definition & Some Auxiliary Problems

We formally define the main problems studied below, along with auxiliary problems whose solutions aid in deriving key results. All definitions are provided in this section for convenience.

n-agent Disk Inspection Problem, \mathcal{S}_n : In this problem, n unit-speed agents (searchers) start from the center of a unit-radius disk. The agents can move freely within the plane of the disk, changing directions without added time costs. For a given trajectory, a point P on the disk's perimeter is said to be inspected if an agent passes through a point A in the plane such that no convex combination of A and P lies within the disk. The first time P is inspected by an agent is its *inspection time*, denoted by $\mathcal{I}(P)$. Feasible solutions to this problem are agents' trajectories that inspect every point on the disk's perimeter. In \mathcal{S}_n , the focus is on minimizing either the worst-case inspection time, $\sup_P \mathcal{I}(P)$, or the average-case inspection time, $\mathbb{E}_P \mathcal{I}(P)$, where the expectation is taken over a uniform distribution of P .

The problem of minimizing $\sup_P \mathcal{I}(P)$ for \mathcal{S}_1 was originally introduced and optimally solved in [46]. Also known as the *shoreline problem with known distance*, it seeks the shortest trajectory of a unit-speed agent to reach a hidden line located at a distance of 1 from the agent. Equivalently, the problem asks for the shortest continuous 1-dimensional curve, with one endpoint at the disk's center, whose convex hull encloses the disk. Minimizing $\sup_P \mathcal{I}(P)$ for \mathcal{S}_n extends this description with n such curves.

For the problem of minimizing $\mathbb{E}_P \mathcal{I}(P)$ in \mathcal{S}_n , the relevant trajectories correspond to deterministic algorithms, evaluated by their average-case performance. Alternatively, these algorithms can be viewed as randomized, where the circle is uniformly rotated before execution. Under this randomized interpretation, the expected inspection time $\mathcal{I}(P)$ is identical for all points P and matches the expected performance of the deterministic algorithm under a uniformly random choice of P . Thus, minimizing $\mathbb{E}_P \mathcal{I}(P)$ can also be framed as minimizing the worst-case (expected) performance of a randomized algorithm.

Single-Agent Partial Disk Inspection Problem, $\mathcal{P}(c)$: Our approach to minimizing $\sup_P \mathcal{I}(P)$ for \mathcal{S}_n is facilitated by examining the single-agent problem $\mathcal{P}(c)$, which involves inspecting an arc of length $c \in [0, 2\pi]$ on the disk's perimeter. Noting that in an optimal solution for \mathcal{S}_n , all agents should conclude their search simultaneously, each agent should inspect an arc of length $2\pi/n$. Thus, \mathcal{S}_n is equivalent to $\mathcal{P}(2\pi/n)$.

Single-Agent Auxiliary Disk Inspection Problem, $\mathcal{A}(k, \theta, c)$: This problem is defined for parameters $k \in \mathbb{N} \cup \{\infty\}$, $\theta < \pi/2$, and $c \geq 2\theta$. It is inspired by optimal (worst-case performance) algorithms for \mathcal{S}_n . Here, a single-agent partial inspection problem is introduced where the agent's starting position is not at the origin but at a carefully selected point outside the disk's interior. This setup enables deriving results also for minimizing $\mathbb{E}_P \mathcal{I}(P)$ for \mathcal{S}_n .

The parameter k designates whether the inspection domain is discrete or continuous, with k specifying the number of discrete inspection points if applicable. The parameter c represents the range of points to be inspected, and θ specifies the agent's initial position. For simplicity, we consider a unit-radius disk centered at the origin in the 2D Cartesian plane, denoted O , with its perimeter parameterized as $\mathcal{P}_t := (\cos t, \sin t)$, where $t \in [0, 2\pi]$.

In $\mathcal{A}(k, \theta, c)$, the agent starts at $(1, \tan \theta)$. When $k = \infty$, the objective is to inspect points P_ϕ with $\phi \in [2\theta, c]$, noting that points P_ϕ in $[0, 2\theta]$ are already inspected due to the agent's initial placement, as we will prove later. When $k \in \mathbb{N}$, the goal is to inspect discrete points $P_i := \mathcal{P}_{\phi_i}$, where

$$\phi_i := 2\theta + \frac{c - 2\theta}{k}i, \quad i = 0, \dots, k.$$

Here, ϕ_i implicitly depends on the fixed values of k , θ , and c . As with \mathcal{S}_n , $\mathcal{A}(k, \theta, c)$ may aim to minimize either the worst-case or average-case inspection time. Later, we will connect and quantify solutions for $\mathcal{A}(\infty, \theta, c)$ and $\mathcal{A}(k, \theta, c)$, ultimately relating them to \mathcal{S}_n for carefully selected values of k , θ , and c based on n .

Single-Agent Trade-off Problem $\mathcal{T}(\lambda)$: With our results for \mathcal{S}_n established, we consider the multi-objective optimization problem of minimizing both worst-case and average-case inspection times with a single agent. Alternatively, we approach bounding the Pareto-optimal set for these objectives by minimizing

$$\lambda \cdot \sup_P \mathcal{I}(P) + (1 - \lambda) \cdot \mathbb{E}_P \mathcal{I}(P),$$

where $\lambda \in [0, 1]$. The trade-off problem $\mathcal{T}(\lambda)$ addresses real-life applications in which minimizing average performance is prioritized, subject to a manageable worst-case bound, such as cases with energy constraints that limit the operational duration of mobile agents.

2.2 Main Results Made Formal & Motivation

In this section we outline our main contributions. The motivating starting point for the present work is a result established by Isbell in 1957.

Theorem 1 ([46]). *The optimal worst case cost to \mathcal{S}_1 is $1 + \sqrt{3} + \frac{7\pi}{6} \approx 6.39724$.*

We generalize the above result by proving, as a warm-up, the following.

Theorem 2. *The optimal worst case cost to \mathcal{S}_n*

$$\begin{cases} 1 + \sqrt{3} + 2\pi/n - 5\pi/6, & \text{if } n = 1, 2 \\ 1/\cos(\pi/n), & \text{if } n \geq 3 \end{cases}$$

The results of Theorem 2 for \mathcal{S}_n , with $n \geq 2$, are also derived as corollaries from the lower bounds in [30] (for $n = 2, 3$) and in [1] for $n \geq 4$. These papers also address the search for a shoreline without knowledge of the distance from the starting point. However, some of the lower bound arguments in these works are independent of the shoreline’s distance from the starting position, despite being based on competitive analysis. In our case, with known distance, we provide an alternative proof specifically designed for the problem where the distance is known. More significantly, we derive our results as corollaries of a solution to the more general problem of inspecting an arc of arbitrary length $c \in [0, 2\pi]$, a result not achieved in prior studies. Indeed, the proof of Theorem 2 follows directly from the broader Theorem 5, which establishes the optimal worst-case solution to the Partial Inspection Problem $\mathcal{P}(c)$ for every $c \in [0, 2\pi]$ and is of independent interest. In particular, for $c \geq 5\pi/6$ we show that an Isbell-type trajectory is the optimal solution to $\mathcal{P}(c)$, generalizing the optimal trajectory for \mathcal{S}_1 in [46] and the optimal trajectory for \mathcal{S}_2 in [30].

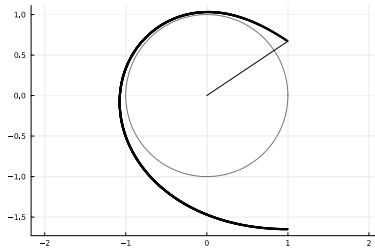
Our next main result pertains to upper bounds for the average-case inspection time to \mathcal{S}_n .

Theorem 3. *\mathcal{S}_n can be solved in average-case inspection time as outlined in the next table.*

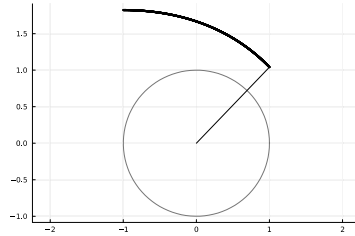
n	1	2	≥ 3
average cost	3.5509015	1.7946051	$\frac{n}{2\pi} \log \left(\frac{1 + \sin \pi/n}{1 - \sin \pi/n} \right)$

Table 1: Upper bounds to the average inspection cost of \mathcal{S}_n . Indicatively, we also get performance equal to $\frac{3 \log(4\sqrt{3}+7)}{2\pi} \approx 1.2576$ and $\frac{2 \log(2\sqrt{2}+3)}{\pi} \approx 1.1222$, for $n = 3, 4$, respectively, while the values continue to drop and asymptotically tend to $1 + \Theta(1/n^2)$.

As before, our results are based on designing efficient average-cost inspection algorithms for the general problem $\mathcal{P}(c)$, $c \in [0, 2\pi]$, which may be of independent interest. The reader is referred to Figure 1 for the derived trajectories minimizing the average-cost inspection time for $n = 1, 2$, corresponding to solutions for $\mathcal{P}(c)$ with $c = \pi$ and $c = 2\pi$. Figure 9 on page 19 displays the optimal trajectories derived for $\mathcal{P}(c)$ for additional values of c .



(a) The trajectory proving the average inspection upper bound to \mathcal{S}_1 .



(b) The trajectory proving the average inspection upper bound to \mathcal{S}_2 .

Fig. 1: Agent's trajectories of Theorem 3 for $n = 1, 2$.

Notably, the naive inspection algorithm for \mathcal{S}_n , where each agent inspects an arc of length $2\pi/n$ along the disk, yields an average inspection cost of $1 + \pi/n$, which is approximately 4.14159 and 2.5708 for $n = 1$ and $n = 2$, respectively. This improvement is substantial for all values of n , and asymptotically, our results show that the average inspection cost converges to $1 + \frac{\pi^2}{6n^2} + o\left(\frac{1}{n^3}\right)$.

In Section 5, we analyze the trade-offs between worst-case and average-case inspection costs for \mathcal{S}_1 , focusing on minimizing the multi-objective function $\{\sup_P \mathcal{I}(P), \mathbb{E}_P \mathcal{I}(P)\}$. This is achieved by minimizing $\lambda \cdot \sup_P \mathcal{I}(P) + (1 - \lambda) \cdot \mathbb{E}_P \mathcal{I}(P)$, for $\lambda \in [0, 1]$. Theorem 2 (originally due to [46] for \mathcal{S}_1) provides the worst-case optimal inspection time for \mathcal{S}_1 as $1 + \sqrt{3} + \frac{7\pi}{6} \approx 6.39724$, while the same trajectory has an average inspection cost of $\frac{5}{2\sqrt{3}} + \frac{91\pi}{144} + \frac{\log(6)}{2\pi} \approx 3.71386$, as shown in Lemma 6.

At the other end, Theorem 3 gives an upper bound on the average inspection cost at 3.5509015, corresponding to a trajectory length of approximately 6.8673829. We are thus motivated to establish upper bounds on average-case performance when the trajectory length varies between 6.39724 and 6.8673829.

To achieve this, we first determine the Pareto curve for the Isbell-type trajectories used in the proof of Theorem 1, parameterized by θ . For suitable values of θ , we compute in Lemma 6 both the worst-case and average-case costs for this family of algorithms, which serve as benchmarks for our subsequent results.

Finally, to improve the upper bounds for the multi-objective inspection problem, we extend our approach to minimize average-case inspection costs. This is accomplished using a discrete trajectory optimized through a Non-Linear Program with carefully selected parameters. The bounds for the Pareto curve of the multi-objective inspection problem are summarized in the following theorem.

Theorem 4. *Single Agent trade-off problem $\mathcal{T}(\lambda)$, where $\lambda \in [0, 1]$ admits inspection trajectories with worst-case cost and average-case cost to \mathcal{S}_1 that are depicted in Figure 2.*

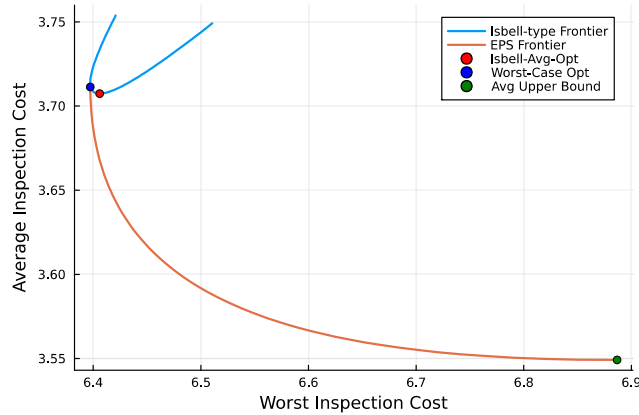


Fig. 2: Our Pareto upper bounds are depicted in orange and are achieved by the Extended-Poly-Segment (EPS) trajectory we define later. The blue line depicts the Pareto Frontier of the Isbell-type trajectories, parameterized by the initial deployment angle θ . The provable worst-case optimal solution and its corresponding average inspection performance are shown as the blue Pareto point. The red Pareto point corresponds to the performance of the Isbell-type trajectory that is average cost optimal. Finally, the green Pareto point is the performance of the EPS-type trajectory with the smallest average inspection cost.

3 Optimal Worst Case Inspection for \mathcal{S}_n

3.1 Some Preliminary Observations

To simplify the notation, we remind the reader of some existing abbreviations and introduce new ones. Throughout our analysis, we will work with a fixed $k \in \mathbb{N}$, and $\theta, c \in [0, 2\pi]$, where $\theta < \pi/2$ and $\theta \leq 2c$. For such fixed k, c , and θ , we define:

$$\phi_i := 2\theta + \frac{c - 2\theta}{k}i, \quad i = 0, \dots, k \quad (1)$$

$$P_i := \mathcal{P}_{\phi_i}, \quad i = 0, \dots, k \quad (2)$$

The values ϕ_i are chosen such that the intervals $[\phi_i, \phi_{i+1}]$ form a (non-disjoint) partition of the interval $[2\theta, c]$, for $i = 0, \dots, k - 1$. Additionally, the points P_i represent the endpoints of the corresponding arcs on the perimeter of the unit disk.

For some $\phi \in [0, 2\pi]$, we also consider the parametric equation of the line $\mathcal{L}_\phi(t)$, which is tangent to the disk at the point \mathcal{P}_ϕ :

$$\mathcal{L}_\phi(t) := \begin{pmatrix} \cos(\phi) \\ \sin(\phi) \end{pmatrix} + t \begin{pmatrix} \sin(\phi) \\ -\cos(\phi) \end{pmatrix}. \quad (3)$$

For the same fixed k, c, θ , we will also need to consider the tangent $\mathcal{L}_\phi(t)$ at $\phi = \phi_i$, hence it is convenient to introduce the abbreviation $L_i(t) := \mathcal{L}_{\phi_i}(t)$, $t \in \mathbb{R}$, $i = 0, \dots, k$.

The following lemma summarizes some important observations pertaining to conditions that guarantee when points on the perimeter of the disk are inspected.

Lemma 1. (a) *An agent at point with polar coordinates (r, ϕ) and $r \geq 1$ inspects all points \mathcal{P}_t that satisfy $|t - \phi| \leq \arccos(1/r)$.*

- (b) For every $\theta \in [0, \pi/2)$, an agent at point $(1, \tan(\theta))$ inspects all \mathcal{P}_t , with $t \in [0, 2\theta]$.
- (c) An agent inspects point \mathcal{P}_ϕ if and only if it lies in the closed halfspace defined by \mathcal{L}_ϕ that does not contain the interior of the unit disk. In particular, an agent residing on any point of \mathcal{L}_ϕ inspects \mathcal{P}_ϕ .
- (d) Consider points $A = \mathcal{L}_\phi(t_1)$ and $B = \mathcal{L}_{\phi+\gamma}(t_2)$ satisfying $\gamma < \pi/2$, $t_1 \geq 0$ and $t_2 \geq \frac{1-\cos(\chi)}{\sin(\chi)}$. Then, for each $\phi \leq \chi \leq \phi + \gamma$, point \mathcal{P}_χ is inspected by some convex combination of A, B . In other words, the movement $A \rightarrow B$, inspects all points \mathcal{P}_χ , with $\chi \in [\phi, \phi + \gamma]$.

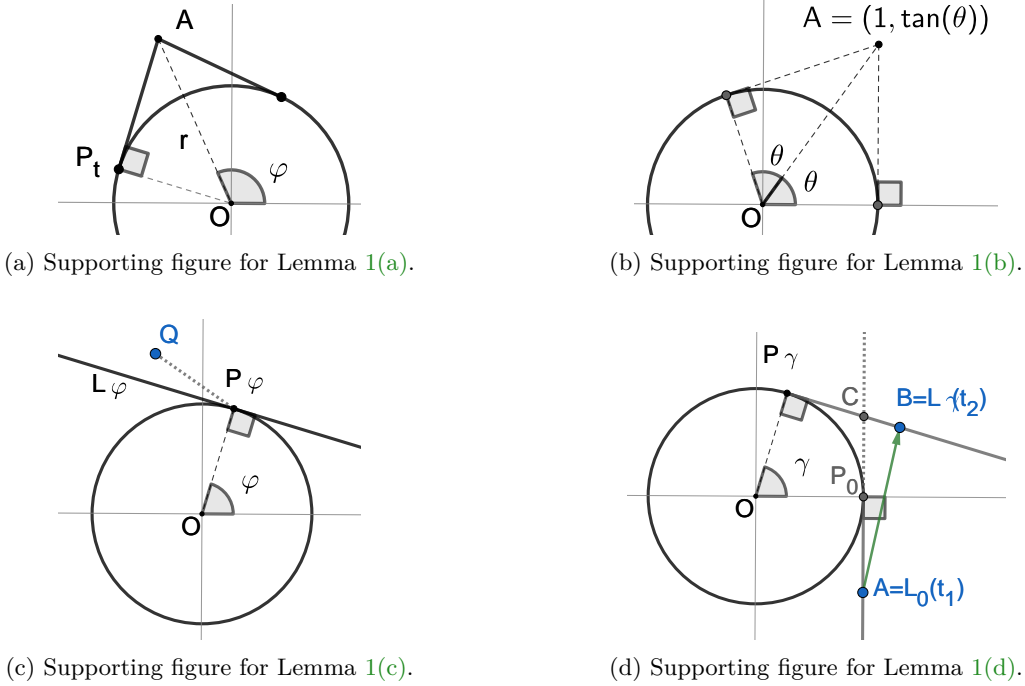


Fig. 3: Supporting figures for Lemma 1.

Proof. (a) See Figure 3a. A point with polar coordinates (r, ϕ) corresponds to Cartesian coordinates $A = r(\cos(\phi), \sin(\phi))$: if $r = 1$, then A is touching the perimeter of the disk, and it only inspects point \mathcal{P}_ϕ . Otherwise, if $r > 1$, we find the two lines that pass from A and that are tangent to the disk. Then, all points in between the tangent points are inspected by point A .

For this, consider an arbitrary point \mathcal{P}_t on the disk. The line passing through A, \mathcal{P}_t is tangent to the disk if and only if $\overrightarrow{OP_t} = (\cos(t), \sin(t))$ is orthogonal to $\overrightarrow{\mathcal{P}_t A} = (r \cos(\phi) - \cos(t), r \sin(\phi) - \sin(t))$. But then, we see that

$$\overrightarrow{OP_t} \cdot \overrightarrow{\mathcal{P}_t A} = r \cos(\phi) \cos(t) + r \sin(\phi) \sin(t) - 1 = r \cos(t - \phi) - 1,$$

and therefore the vectors are orthogonal exactly when $t = \phi \pm \arccos(1/r)$, as wanted.

- (b) See Figure 3b. We have that $\|(1, \tan(\theta))\| = 1/\cos(\theta)$, which also implies that the angle of the polar coordinates of the point is θ . Overall, by Lemma 1(a), an agent at polar coordinates $(1/\cos(\theta), \theta)$ inspects all points \mathcal{P}_t satisfying $|t - \theta| \leq \arccos(\cos(\theta))$, that is all $t \in [0, 2\theta]$.

- (c) See Figure 3c. If an agent lies at point Q in the closed halfspace defined by \mathcal{L}_ϕ not containing the interior of the unit disk, then no convex combination of Q, \mathcal{P}_ϕ is in the interior of the disk, hence she inspects \mathcal{P}_ϕ .

For the other direction, assume that an agent inspects point \mathcal{P}_ϕ from point Q . Note that \mathcal{P}_ϕ cannot coincide with Q . If Q is not in the closed halfspace not containing the disk, then the ray (halfline) starting from \mathcal{P}_ϕ and passing through Q must intersect the disk, contradicting that the agent inspects \mathcal{P}_ϕ .

- (d) See Figure 3d. By rotating by $-\phi$, we may assume that $\phi = 0$, hence $A = \mathcal{L}_0(t_1)$ and $B = \mathcal{L}_\gamma(t_2)$ for $t_1 \geq 0$ and $t_2 \geq \frac{1-\cos(\chi)}{\sin(\chi)}$. By Lemma 1(c), we have that A inspects \mathcal{P}_0 and B inspects \mathcal{P}_γ . Points D that are convex combinations of A, B inspect points \mathcal{P}_χ , with $\chi \in [\phi, \phi + \gamma]$, unless D is less than 1 away from the origin, or in other words, unless segment AB intersects at two distinct points the perimeter of the circle (and hence containing a point in the interior of the circle). We identify the value of t_2 for which segment AB intersects once the circle (at point C in Figure 3d. For this we observe that the equation of line $\mathcal{L}_0(t)$ simplifies to $x = 1$, whereas $\mathcal{L}_\gamma(t) = (\cos(\chi), \sin(\chi)) + t(\sin(\chi), -\cos(\chi))$. We conclude that $\mathcal{L}_\gamma(t)$ intersects $x = 1$ when $(\mathcal{L}_\gamma(t))_1 = 1$, that is, when $\cos(\chi) + t \sin(\chi) = 1$, giving rise to the threshold promised in the statement of the lemma. \square

By Lemma 1(c), \mathcal{P}_ϕ is inspected if an agent lies in the halfspace defined by $\mathcal{L}_\phi(t)$ that does not contain the disk. Therefore, unless an agent is not already in the halfspace of $\mathcal{L}_\phi(t)$ not containing the disk, $\mathcal{I}(\mathcal{P}_\phi)$ is also equal to the first time an agent hits line $\mathcal{L}_\phi(t)$.

3.2 Solving \mathcal{S}_n Using the Partial Inspection Problem $\mathcal{P}(c)$.

The following theorem establishes the optimal worst-case cost for solving the partial inspection problem $\mathcal{P}(c)$. Clearly, $\mathcal{P}(2\pi)$ is equivalent to the problem \mathcal{S}_1 , and indeed, the case $c = 2\pi$ and the corresponding optimal result (see Theorem 1, first proved in [46]) are included in the statement below.

Theorem 5. *The optimal worst case inspection cost to $\mathcal{P}(c)$ is*

$$\begin{cases} \frac{1}{\cos(c/2)}, & \text{if } 0 \leq c \leq \frac{2\pi}{3}, \\ 1 - 2\cos(c), & \text{if } \frac{2\pi}{3} < c \leq \frac{5\pi}{6}, \\ 1 + \sqrt{3} + c - \frac{5\pi}{6}, & \text{if } \frac{5\pi}{6} < c \leq 2\pi. \end{cases}$$

Proof. Without loss of generality, the points to be inspected are all points on the arc $\mathcal{A} = \{\mathcal{P}_\phi : \phi \in [0, c]\}$. Hence, the optimal inspection trajectory is identified by the curve C (of minimum length), with one endpoint at the origin O , and whose convex closure contains \mathcal{A} .

The reader may consult Figure 5. Since the agent initially lies at the origin, she does not inspect any points. Since C is continuous and by Lemma 1(c), the curve C must intersect \mathcal{L}_0 , say at point $A_0 = \mathcal{L}_0(t_0)$, and \mathcal{L}_c at point $A_c = \mathcal{L}_c(t_c)$. Without loss of generality, we assume that A_0 is the first to be hit, and that $t_0 \leq 0$ and $t_c \geq 0$. Because C is of minimum length, the curve must start with the line segment OA_0 .

Next, we use the main technical contribution of [46], which states that the curve C must be convex about the origin O . As a result, C is a convex curve that starts with the segment OA_0 , ends at point A_c . Moreover, the (sub)curve with endpoints A_0 and A_c , call it C' , is the minimum convex curve around O that does not intersect the interior of the disk.

Let D denote the point on C' which is the last (moving from A_0 to A_c) to lie on the perimeter of the disk, or $D = A_0$ if no such point exists. Again, by the minimality (of length) of C' , DA_c

must be perpendicular to line \mathcal{L}_c . Finally, if C' does intersect the perimeter of the disk, let D' denote the first such point (moving from A_0 to A_c). Again, by the minimality of C' , the curve should start as the line segment A_0D' , which by the convexity of the curve C' should not intersect the interior of the disk. Moreover, the segment A_0D' should be tangent to the disk (at D'), as otherwise, one could choose a convex combination A'_0 of A_0 and \mathcal{P}_ϕ such that A_0D' is tangent to the disk at D' . Furthermore, by the triangle inequality, the length of $OA'_0 + A'_0D'$ would be less than that of $OA_0 + A_0D'$, contradicting the minimality of C' . To that end, note also that the portion of C' between D' and D must lie on the perimeter of the disk forming an arc.

Next we identify all curves (inspection trajectories) that comply with the above characteristics. We quantify point A_0 by $\theta \in [0, \pi/2)$, such that $A_0 = (1, \tan(\theta))$, where also $\theta \leq c/2$. We distinguish two cases as to whether curve C' has at most one point on the perimeter of the disk (hence C has at 1 or 2), or infinitely many. For each of these cases, we describe a family of curves, type-1 and type-2, parameterized by θ , and applicable only under conditions of c, θ .

Type-1 curves (see Figure 5a) intersect the perimeter of the disk in 1 or 2 points. Hence for point $A_0 = (1, \tan(\theta))$ and the end point $A_c \in \mathcal{L}_c$ of C , we have that A_0A_c is perpendicular to \mathcal{L}_c . This implies that $0 \leq c \leq 3\pi/2$, and that $2\theta \geq c - \pi/2$. The cost of that trajectory equals $OA_0 + A_0A_c$, where $OA_0 = 1/\cos(\theta)$. In order to find A_0A_c , draw a line parallel to \mathcal{L}_c , passing through the origin, intersecting A_0A_c at point K . Clearly, $KA_c = 1$, in triangle OKA_0 , we have that $\sin(c - \theta - \pi/2) = A_0K/OA_0$, and hence $A_0K = \sin(c - \theta)/\cos(\theta)$. Overall, the length of that trajectory becomes

$$f_1(\theta) := 1/\cos(\theta) + \sin(c - \theta - \pi/2)/\cos(\theta) + 1.$$

Type-2 (Isbell-type) curves (see Figure 5b) intersect the perimeter of the disk in infinitely many points. In other words, trajectory is made up by line segment OA_0 , then tangent line segment A_0D' (where $D' = \mathcal{P}_{2\theta}$), then arc $D'D$, and the line segment DA_c (tangent to the disk at point $D = \mathcal{P}_{c-\pi/2}$ and) perpendicular to \mathcal{L}_c . For this configuration to be well defined, we need $\theta \leq c/2 + \pi/2$, as well as $c \geq \pi/2$. Note that $A_0D' = A_0P_0 = \tan(\theta)$, the length of the arc $D'D$ equals $c - \pi/2 - 2\theta$, while $DA_c = 1$. But then, the length of the curve, becomes

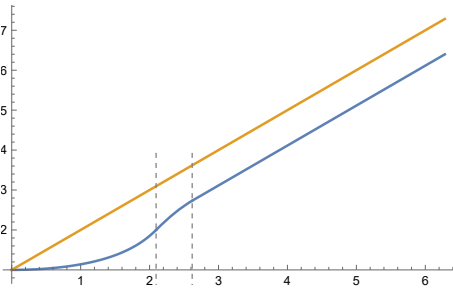
$$f_2(\theta) = 1/\cos(\theta) + \tan(\theta) + c - \pi/2 - 2\theta + 1.$$

It follows that when $c \leq \pi/2$ only type-1 curves are applicable, when $\pi/2 \leq c \leq 3\pi/2$ both type-1 and type-2 curves are applicable, and when $c \geq 3\pi/2$ only type-2 curves are applicable.

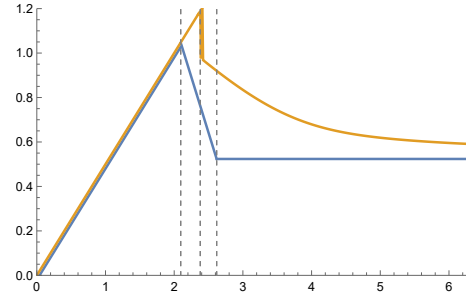
Lemmata 7 and 8 in Section A.1 minimize $f_1(\theta)$ and $f_2(\theta)$. Therefore, for each $c \in [0, \pi/2]$ for which only type-1 curves are applicable, their optimal length is $f_1(c/2) = 1/\cos(c/2)$. Similarly, for each $c \in [3\pi/2, 2\pi]$ for which only type-2 curves are applicable, their optimal length is $f_2(\pi/6) = \sqrt{3} + c - 5\pi/6 + 1$. For the remaining values of $c \in [\pi/2, 3\pi/2]$, we need to compare f_1, f_2 , which is done in Lemma 9 in Section A.1, concluding the statement of the theorem. \square

A visualization of Theorem 5 is provided in Figure 4. To prove Theorem 5 for $\mathcal{P}(c)$, we identify the shortest curve, C , that inspects all points along the arc of length c . The proof distinguishes between two types of curves: Type-1 (Figure 5a), which intersects the disk perimeter at one or two points and applies when $0 \leq c \leq 3\pi/2$, and Type-2 (Isbell-type) curves (Figure 5b), which intersect the perimeter infinitely and apply when $c \geq \pi/2$. For each configuration, we derive conditions for minimal length based on convexity constraints around the disk, ensuring that C fully covers the arc while minimizing total distance. The detailed derivation of these cases is provided in the appendix.

We note that the optimal worst case inspection cost to $\mathcal{P}(c)$ is continuous at $c = 2\pi/3$ and at $c = 5\pi/6$ with corresponding worst case costs equal to 2 and $1 + \sqrt{3}$, respectively. Moreover, and not surprisingly, it is easy to see that the cost is monotonically increasing in c .

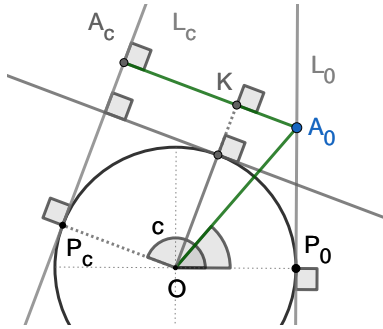


(a) The worst-case optimal inspection cost for solving the partial problem $\mathcal{P}(c)$ (blue curve), as a function of c (see Theorem 5). The dotted lines represent the values of c at which the piecewise-defined cost function changes its formula. The yellow curve is given for comparison, and represents $1 + c$ which is the cost of the naive algorithm for solving $\mathcal{P}(c)$.

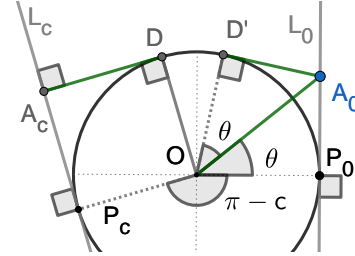


(b) The worst-case optimal deployment angle θ (in blue) of $\text{EPS}(\theta, t_1, \dots, t_k)$ is shown as a function of the arc length c to be inspected in $\mathcal{P}(c)$ (see Theorem 5). The yellow plot illustrates the behavior of the angle $\theta = \theta(c)$ for the inspection algorithm $\text{EPS}(\theta, t_1, \dots, t_k)$, when the parameters are chosen to optimize the average inspection cost for $\mathcal{P}(c)$, see Theorem 8. The gray dotted lines represent transition thresholds for the optimizers θ in the two cases.

Fig. 4: Visualization of the results in Theorem 5, and Theorem 8.



(a) Type-1 curves (in green) for solving $\mathcal{P}(c)$, applicable when $0 \leq c \leq 3\pi/2$ and $2\theta \geq c - \pi/2$.



(b) Type-2 (Isbell-type) curves (in green) for solving $\mathcal{P}(c)$, applicable when $\pi/2 \leq c \leq 2\pi$ and $2\theta \leq c - \pi/2$.

Fig. 5: Trajectories achieving the worst-case optimal inspection cost to $\mathcal{P}(c)$ as per Theorem 5.

As an immediate corollary we obtain the optimal worst case cost for the general inspection problem \mathcal{S}_n , as stated in Theorem 2.

Proof (of Theorem 2). Consider any partition of the perimeter of the disk that assigns points to inspect to the n agents. This defines a number of arcs covering the perimeter of the disk, each labeled according to the assigned agents. It is easy to see that the arcs in the partition can be rearranged (each agent still being assigned the same total portion of the disk) so that those with the same label are contiguous, without increasing the cost.

Hence, each agent needs to inspect a contiguous arc. Next, we claim that all agents inspect arcs of the same length. If not, we could slightly decrease the largest arc and slightly increase the

smallest arc. From Theorem 5, the optimal cost for covering any arc of length c is monotonically increasing in c , and thus this adjustment would reduce the overall inspection cost.

We conclude that each agent inspects an arc of length $c = 2\pi/n$. The claim of the theorem follows from Theorem 5, which describes the worst-case optimal cost for inspecting an arc of length c , for every $c \in [0, 2\pi]$. \square

4 Average-Case Inspection Upper Bounds for \mathcal{S}_n

4.1 Discrete Inspection Algorithms for $\mathcal{A}(k, \theta, c)$ and $\mathcal{P}(c)$

In this section, we introduce and analyze the trajectory (Algorithm) POLYSEGMENT for solving $\mathcal{A}(k, \theta, c)$ and the trajectory (Algorithm) EXTENDEDPOLYSEGMENT, which, under certain conditions, will solve the 1-agent partial inspection problem $\mathcal{P}(c)$ and eventually the n -agent inspection problem \mathcal{S}_n .

Recall that $\theta \in [0, \pi/2)$, and $c \in [0, 2\pi]$, with $c \geq 2\theta$. We fix these constants and also fix $k \in \mathbb{N}$, i.e., for the description of the trajectory, we require k to be finite. The algorithm will be parameterized by (t_1, \dots, t_k) , where $t_i \in \mathbb{R}$. Recall that in $\mathcal{A}(k, \theta, c)$, we need to inspect points P_i with angular values $\phi_i := 2\theta + \frac{c-2\theta}{k}i$, $i = 0, \dots, k$. Note that the remaining of the necessary notation was introduced earlier in Section 3.1. Along with the algorithm description below, the reader may also consult Figure 6 on page 13.

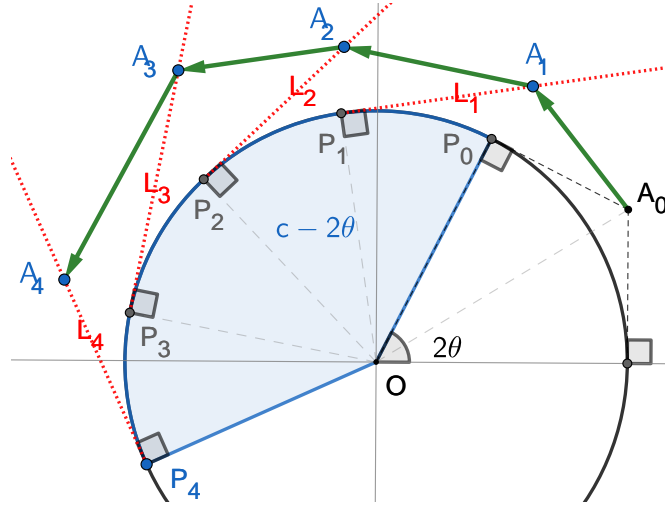


Fig. 6: In this example $k = 4$, and we demonstrate how $\text{PS}(t_1, \dots, t_4)$ is feasible to $\mathcal{A}(4, \theta, c)$. The disk segment of arc length $c - 2\theta$, whose perimeter needs to be inspected, is depicted as the light blue sector. The tangent lines $L_i(t)$ are depicted as dotted red lines, where only the halflines corresponding to $t \geq 0$ are shown. We let $A_0 = (1, \tan(\theta))$, and we note that there exists t_0 such that $A_0 = \mathcal{L}_{\phi_0}(t_0)$, where $\phi_0 = 2\theta$. For $i = 1, 2, 3, 4$, the points A_i are obtained as $A_i = L_i(t_i)$ with $t_i > 0$. By inspection, we see that the choice of t_i makes the trajectory $A_0 \rightarrow A_1 \rightarrow A_2 \rightarrow A_3 \rightarrow A_4$ feasible to $\mathcal{A}(4, \theta, c)$ as well as to $\mathcal{A}(\infty, \theta, c)$. Feasibility to $\mathcal{A}(\infty, \theta, c)$ will be examined later, and we stress that it is not sufficient to have $t_i > 0$.

Algorithm 6 (PolySegment(t_1, \dots, t_k)) Given k, θ, c with $\theta < \pi/2$, $c \geq 2\theta$, we set $A_0 := (1, \tan(\theta))$, and $A_i := L_i(t_i)$. Then, the trajectory is defined by the movement between points $A_0 \rightarrow A_1 \rightarrow \dots \rightarrow A_k$.

For fixed k, θ, c , our goal will be to determine optimal values for (t_1, \dots, t_k) so as to minimize the average case performance to $\mathcal{A}(k, \theta, c)$. For the ease of notation, we will refer to the trajectory as $\text{PS}(t_1, \dots, t_k)$. Next we comment on the algorithm's feasibility and compute its average case inspection cost.

Lemma 2. For every $k \in \mathbb{N}$ and for all $t_i \in \mathbb{R}$, trajectory $\text{PS}(t_1, \dots, t_k)$ is feasible to $\mathcal{A}(k, \theta, c)$. Moreover, trajectory $\text{PS}(t_1, \dots, t_k)$ has worst case cost $\sum_{j=1}^k \|A_{j-1}A_j\|$ and average case cost

$$\frac{1}{k+1} \sum_{j=1}^k (k-j+1) \|A_{j-1}A_j\|.$$

Proof. By Lemma 1(c), an agent on $L_i(t)$ inspects point P_i , and we have one such $A_i = L_i(t_i)$, for each $i = 0, \dots, k$. Therefore, trajectory $\text{PS}(t_1, \dots, t_k)$ is indeed feasible.

The length of the trajectory equals $\sum_{j=1}^k \|A_{j-1}A_j\|$, and since every point P_i is inspected no later than when the agent reaches A_i , it follows that no point is inspected later than the length of the trajectory, concluding the claim about the worst case.

Next we calculate the average inspection cost of points P_0, P_1, \dots, P_k , deriving this way the average case analysis. For this, we calculate the inspection time $\mathcal{I}(P_i)$ for each P_i , and recall that by Lemma 1(b) we have that $\mathcal{I}(P_0) = 0$. Also, we see that $\mathcal{I}(P_i) \leq \sum_{j=1}^i \|A_{j-1}A_j\|$, for $i = 1, \dots, k$ and hence the average inspection time is

$$\frac{1}{k+1} \sum_{i=0}^k \mathcal{I}(P_i) \leq \frac{1}{k+1} \sum_{i=1}^k \sum_{j=1}^i \|A_{j-1}A_j\| = \frac{1}{k+1} \sum_{i=1}^k (k-i+1) \|A_{i-1}A_i\|.$$

□

Trajectory $\text{POLYSEGMENT}(t_1, \dots, t_k)$ will be eventually used to derive upper bounds to \mathcal{S}_n . Below we extend the trajectory, and we quantify its performance assuming it is feasible for the continuous partial inspection problem. In that direction, we present trajectory (algorithm) $\text{EXTENDEDPOLYSEGMENT}$ for solving $\mathcal{P}(c)$.

Algorithm 7 (ExtendedPolySegment(θ, t_1, \dots, t_k))

Given $c \in [0, 2\pi]$, $k \in \mathbb{N}$ and $\theta \leq \{c/2, \pi/2 - \epsilon\}$ for some $\epsilon > 0$, we set $A_0 := (1, \tan(\theta))$, and $A_i := L_i(t_i)$.¹ Then, the trajectory of the agent is defined by the movement between points $O \rightarrow A_0 \rightarrow A_1 \rightarrow \dots \rightarrow A_k$, where O is the center of the disk.

For notational convenience, we will refer to the algorithm above as $\text{EPS}(\theta, t_1, \dots, t_k)$. Next, we describe its performance on $\mathcal{P}(c)$ as a function of its performance on the discrete problem, assuming also that it is feasible for the problem. We will introduce the feasibility conditions later.

Lemma 3. Let $k \in \mathbb{N}$ and $\theta \leq \{c/2, \pi/2 - \epsilon\}$ for some $\epsilon > 0$. Suppose also that $\text{PS}(t_1, \dots, t_k)$ ² is feasible to $\mathcal{A}(\infty, \theta, c)$ with worst case cost and the average case inspection cost equal to s_1 and s_2 , respectively. Then,

¹ Recall that the definition of lines L_i is tailored to the fixed k, θ, c .

² Note that the trajectory points are tailored to the fixed values of k, θ, c .

which is based on that $\int \frac{1}{\cos(\phi)} d\phi = \text{ArcCoth}(\sin(\phi))$. □

We are now ready to introduce the feasibility conditions of the discrete inspection algorithm for the continuous inspection problems, as well as to relate the performance of the algorithm for the discrete and continuous inspection problems. As a reminder, the parameter k quantifies the refinement of the continuous space into a discrete set of points to be inspected. The value of k that we will eventually use is on the order of thousands, and the higher it is, the better our results for the continuous problem. The requirement in the lemma that $k \geq 5$ becomes apparent only in the proof, where we need the points to be inspected to be strictly less than $\pi/2$ apart.

Lemma 4. *Consider $k \geq 5 \in \mathbb{N}$ and $t_i \in \mathbb{R}$, satisfying $t_i \geq \frac{1 - \cos(\frac{c-2\theta}{k})}{\sin(\frac{c-2\theta}{k})}$, $i = 1, \dots, k$. Then, trajectory $PS(t_1, \dots, t_k)$ is feasible to $\mathcal{A}(\infty, \theta, c)$. Moreover, if s is the average case cost for the same trajectory to $\mathcal{A}(k, \theta, c)$, then the average case cost to $\mathcal{A}(\infty, \theta, c)$ is at most $(1 + \frac{1}{k})s$.*

Proof. Fix $k \geq 5$ and t_1, \dots, k satisfying $t_i \geq \tan(\frac{c-2\theta}{k})$, $i = 1, \dots, k$ along with the trajectory $PS(t_1, \dots, t_k)$ which can be represented as $A_0 \rightarrow A_1 \rightarrow \dots \rightarrow A_k$. First, we argue that the trajectory is feasible to $\mathcal{A}(\infty, \theta, c)$. For this, note that if $c = 2\theta$, then by Lemma 1(b) the only point that needs to be inspected, i.e. $\mathcal{P}_{2\theta}$, is indeed inspected due to A_0 . Hence, we may assume that $c > 2\theta$. We need to argue that all points \mathcal{P}_ϕ , where $\phi \in [2\theta, c]$, are inspected. For this, observe that the interval can be partitioned into the (non-disjoint) intervals $[\phi_{i-1}, \phi_i]$ with $\phi_i - \phi_{i-1} = \frac{c-2\theta}{k} \leq \frac{2\pi}{5} < \pi/2$. Therefore by Lemma 1(d), each such subinterval is inspected by the movement $A_{i-1} \rightarrow A_i$, where $i = 1, \dots, k$. Hence the trajectory is feasible to $\mathcal{A}(\infty, \theta, c)$.

Next we provide an upper bound to the cost of the trajectory, as a function of the average case cost of the same trajectory to $\mathcal{A}(k, \theta, c)$. For this, we recall from the argument above that for every $\phi \in [\phi_{i-1}, \phi_i]$, point \mathcal{P}_ϕ is inspected during the movement $A_{i-1} \rightarrow A_i$, and hence for these points we have that $\mathcal{I}(\mathcal{P}_\phi) \leq \sum_{j=1}^i \|A_{j-1}A_j\|$. Noting also that $\mathcal{I}(\mathcal{P}_\phi) > 0$ for all $\phi \in [2\theta, c]$, allows to calculate the average cost of the trajectory to $\mathcal{A}(\infty, \theta, c)$ (as a function of the average case performance s to $\mathcal{A}(k, \theta, c)$) as

$$\begin{aligned} \frac{1}{c-2\theta} \int_{2\theta}^c \mathcal{I}(\mathcal{P}_\phi) d\phi &= \frac{1}{c-2\theta} \sum_{i=1}^k \int_{\phi_{i-1}}^{\phi_i} \mathcal{I}(\mathcal{P}_\phi) d\phi \\ &\leq \frac{1}{c-2\theta} \sum_{i=1}^k \int_{\phi_{i-1}}^{\phi_i} \sum_{j=1}^i \|A_{j-1}A_j\| d\phi \\ &= \frac{1}{c-2\theta} \sum_{i=1}^k (\phi_i - \phi_{i-1}) \sum_{j=1}^i \|A_{j-1}A_j\| \\ &= \frac{1}{c-2\theta} \sum_{i=1}^k (\phi_k - \phi_{i-1}) \|A_{i-1}A_i\|. \end{aligned} \tag{4}$$

Finally, we see that

$$\phi_k - \phi_{i-1} = c - \left(2\theta + \frac{c-2\theta}{k}(i-1) \right) = (c-2\theta) \left(1 - \frac{i-1}{k} \right)$$

Therefore, continuing from (4), we see that an upper bound to average case performance to $\mathcal{A}(\infty, \theta, c)$ is

$$\sum_{i=1}^k \left(1 - \frac{i-1}{k} \right) \|A_{i-1}A_i\| = \frac{1}{k} \sum_{i=1}^k (k-i+1) \|A_{i-1}A_i\| = \frac{k+1}{k}s,$$

where the last equality follows from Lemma 2. \square

4.2 Upper Bounds to the Average Case Inspection of $\mathcal{P}(c)$ and \mathcal{S}_n

In this section we introduce a Non Linear Program ($\text{NLP-avg}(k, c, \epsilon)$) for finding a feasible EXTENDEDPOLYSEGMENT trajectory to $\mathcal{P}(c)$ and for minimizing its average case performance. The algorithm also takes as input some $k \geq 5$ and $c \in [0, 2\pi]$, ensuring that the points to be inspected on the disk's perimeter are less than $\pi/2$ apart. In fact, the values of k we use are on the order of thousands, and the higher they are, the better our results for the continuous problem.

For fixed k, θ , and using the notation introduced at the beginning of Section 3.1, we write explicit formulas for points A_0, A_1, \dots, A_k used by algorithm $\text{EPS}(\theta, t_1, \dots, t_k)$ (see the formal description in 7) with respect to the NLP variables $\theta \in \mathbb{R}$ and $t \in \mathbb{R}^k$. For this, we also recall that $A_i = L_{\phi_i}(t_i)$ for $i = 1, \dots, k$, and that $A_0 = (1, \tan(\theta))$.

Therefore, it is easy to see that

$$\begin{aligned} \|A_0 A_1\|^2 &= (-1 + c'_{\theta,k} + s'_{\theta,k} t_1)^2 + (-s'_{\theta,k} + c'_{\theta,k} t_1 + \tan(\theta))^2, \\ \|A_i A_{i+1}\|^2 &= 2 - 2c_{\theta,k} + 2s_{\theta,k} t_i + t_i^2 - 2(s_{\theta,k} + c_{\theta,k} t_i) t_{i+1} + t_{i+1}^2, \end{aligned}$$

where

$$\begin{aligned} c'_{\theta,k} &= \cos((2(\pi + (-1 + k)\theta))/k) \\ s'_{\theta,k} &= \sin((2(\pi + (-1 + k)\theta))/k), \\ c_{\theta,k} &= \cos((2(\pi - \theta))/k), \\ s_{\theta,k} &= \sin((2(\pi - \theta))/k). \end{aligned}$$

We are now ready to write down the promised NLP, which, based on the observations above, is defined on the variables $t \in \mathbb{R}^k$ and $\theta \in \mathbb{R}$. The value of $\epsilon > 0$ is provided as part of the input and is chosen to be sufficiently small, ensuring that the expressions are well-defined over the domain of θ .

$$\begin{aligned} \min_{t \in \mathbb{R}^k, \theta \in \mathbb{R}} \quad & \frac{1}{c} \log \left(\frac{1 + \sin(\theta)}{1 - \sin(\theta)} \right) + \left(1 + \frac{1}{k} \right) \left(1 - \frac{2\theta}{c} \right) \left(\|OA_0\| + \frac{1}{k+1} \sum_{i=0}^{k-1} (k-i) \|A_i A_{i+1}\| \right) \\ & \text{(NLP-avg}(k, c, \epsilon)) \\ \text{s.t.} \quad & \sin \left(\frac{c-2\theta}{k} \right) t_i \geq 1 - \cos \left(\frac{c-2\theta}{k} \right), \quad i = 1, \dots, k, \\ & 0 \leq \theta \leq \min \left\{ \frac{(1-\epsilon)c}{2}, \frac{\pi}{2} - \epsilon \right\}. \end{aligned}$$

Lemma 5. *Fix $\epsilon > 0$, small enough. For any feasible solution $(\theta, t) \in \mathbb{R}^k$ to $(\text{NLP-avg}(k, c, \epsilon))$ with $k \geq 5$, $\text{EPS}(\theta, t_1, \dots, t_k)$ is a feasible inspection algorithm to $\mathcal{P}(c)$. Moreover the objective to the NLP quantifies the corresponding average case cost of the algorithm.*

Proof. For a solution $(\theta, t) \in \mathbb{R}^k$ to $(\text{NLP-avg}(k, c, \epsilon))$, we observe that

$$t_i \geq \left(1 - \cos \left(\frac{c-2\theta}{k} \right) \right) / \sin \left(\frac{c-2\theta}{k} \right),$$

for $i = 1, \dots, k$. By Lemma 4 the trajectory $\text{PS}(t_1, \dots, t_k)$ is feasible to $\mathcal{A}(\infty, \theta, c)$, and if its average case cost to $\mathcal{A}(k, \theta, c)$ equals s , then the average case cost to $\mathcal{A}(\infty, \theta, c)$ is at most $(1 + \frac{1}{k})s$.

Then, by Lemma 3, we obtain that $\text{EPS}(\theta, t_1, \dots, t_k)$ is also feasible to $\mathcal{P}(c)$, with overall cost $\frac{1}{c} \log \left(\frac{1 + \sin(\theta)}{1 - \sin(\theta)} \right) + (1 + \frac{1}{k}) (1 - \frac{2\theta}{c}) s$. Finally, Lemma 2 computes quantity s , which results to the objective of $(\text{NLP-avg}(k, c, \epsilon))$, as promised. \square

We are ready to provide upper bounds to the average inspection cost for $\mathcal{P}(c)$.

Theorem 8. $\mathcal{P}(c)$ admits average inspection cost solution as depicted in Figure 8.

Proof (of Theorem 8). For c from 0.01 up to 2π and with step size 0.01, we compute a numerical solution to $(\text{NLP-avg}(k, c, \epsilon))$ with $k = 1000$ and $\epsilon = 10^{-3}$, and we apply Lemma 5. The numerical solutions were obtained using Julia's JuMP and Ipopt [23,31], which use an interior point method for solving NLPs and terminate with a certificate of local optimality. Hence, even though a general proof of global optimality eludes us, the reported results are provably locally optimal.

It is important to note that all upper bounds were obtained by trajectories $\text{EPS}(\theta, t_1, \dots, t_k)$, which were originally designed for the discrete problem of inspecting $\Theta(k)$ disk points. Figure 4b on page 12 shows the reported (minimizer) deployment angle $\theta = \theta(c)$, which exhibits discontinuity around $c \approx 2.39$. For all values of the reported optimizer $\theta(c)$, we see that the constraint $\theta \leq \min\{(1 - \epsilon)c/2, \pi/2 - \epsilon\}$ is satisfied with slack for $c \geq 2.39$, and hence the value of ϵ does not affect the optimizer (also ϵ was introduced only for technical reasons in order to be able to solve the NLP) for these values of c . For $c \leq 2.39$, the constraint $\theta \leq (1 - \epsilon)c/2$ becomes tight, and then we report the abstract average inspection cost

$$\frac{1}{c} \log \left(\frac{1 + \sin(c/2)}{1 - \sin(c/2)} \right),$$

which we obtain by using $\theta = c/2$ in Lemma 3, part (c). The latter corresponds to the average inspection cost of algorithm $\text{EPS}(c/2, t_1, \dots, t_k)$, where the algorithm's trajectory simplifies to $O \rightarrow A = (1, \tan(c/2))$, and hence the value of k is irrelevant.

Notably, we also observe a discontinuity in the reported average inspection cost at $c = 2.39$ (by an additive term of less than 10^{-3}). This is because the analysis for $c \geq 2.39$ is formal and abstract, whereas for smaller values of c , we rely on numerical computations, in which explicitly, we pay an additional factor of $1 + 1/k$ in the objective as mandated by Lemma 4, and which is the result of converting a trajectory that was originally designed for the discrete inspection problem to the continuous inspection problem.

Finally, it is interesting to observe that there is no value of c for which the optimizers $t_i = t_i(c)$ are close to being tight to the required lower bound of $(1 - \cos(\frac{c-2\theta}{k})) / \sin(\frac{c-2\theta}{k}) = O(1/k)$. Indeed, $\min_i t_i(c)$ is decreasing in c , and for $c = 2\pi$, we find that $\min_i t_i \geq 0.2$.

We display some optimizers $t \in \mathbb{R}^k$ for certain values of c in Figure 13 on page 29 and in Figure 14 on page 30, where we see that they are bounded away from 0. The corresponding inspection trajectories, which are far from touching the perimeter of the disk, are depicted in Figure 1 (on page 7), and in Figure 9 (on page 19). \square

We conjecture that our reported average inspection times are optimal. Interestingly, from our numerical results, we see that the reported average inspection cost is eventually very close to be linear, i.e. it is well approximated by $0.5395026c + 0.1637722$ for $c \geq 4.3$. Some indicative and notable trajectories solving $\mathcal{P}(c)$ and proving Theorem 8 are those corresponding to $c = 2\pi$ and $c = \pi$, see Figure 1 on page 7, and to $c = i\frac{\pi}{4}$ for $i = 5, 6, 7$, see Figure 9.

We are now ready to prove Theorem 3.

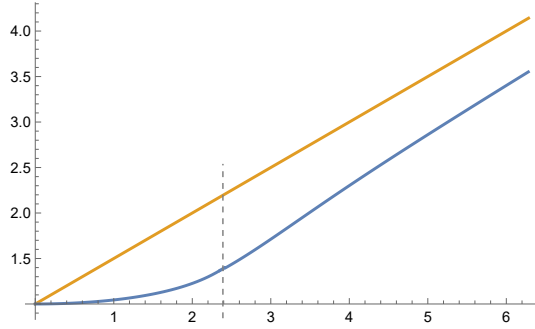


Fig. 8: The reported average inspection cost (in blue) of algorithm $\text{EPS}(\theta, t_1, \dots, t_k)$ as per Theorem 8. For values $c \leq 2.39$, our solution admits an analytic formula for the average cost. For comparison, we also display in yellow the performance $1 + c/2$ of the plain-vanilla randomized algorithm.

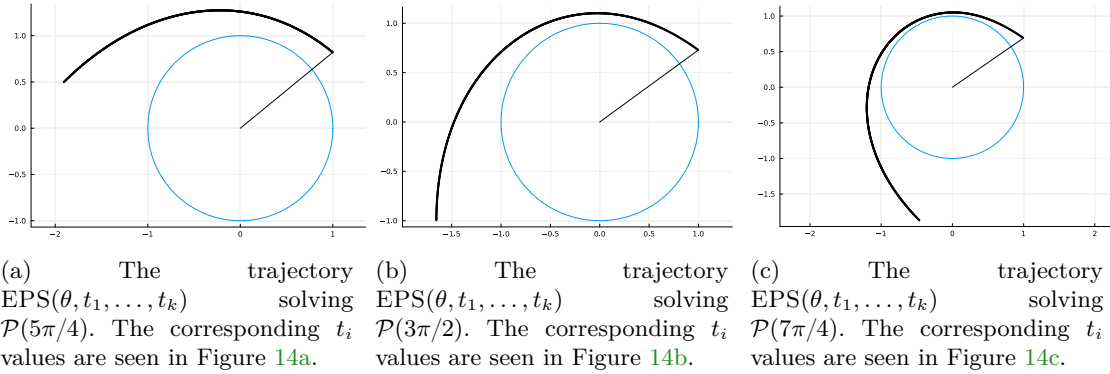


Fig. 9: Trajectories for minimizing the average inspection cost for $\mathcal{P}(c)$, $c = i\frac{\pi}{4}$, where $i = 5, 6, 7$.

Proof (of Theorem 3). The upper bounds on the average inspection cost for \mathcal{S}_n are obtained from the upper bounds of $\mathcal{P}(c)$ in Theorem 8, by setting $c = 2\pi/n$. Since all agents are identical, each is assigned an arc of length $2\pi/n$ to inspect, and the n agents' trajectories are obtained by rotating one agent's trajectory by an angle of $2\pi/n$, $n - 1$ times.

We note that for $n \geq 3$ agents, the length $c = c(n)$ of the arc that each agent inspects satisfies $c \leq 2.39$, and as such the inspection trajectories we report have average cost $\frac{1}{c} \log \left(\frac{1 + \sin(c/2)}{1 - \sin(c/2)} \right)$, as per Lemma 3, part (c). More specifically, one agent's trajectory is given by the line segment OA , where $A = (1, \tan(c/2))$, and all other trajectories are rotations of this segment by $2\pi/n$.

It follows that only for $n = 1, 2$ are the trajectories more elaborate, requiring the numerical solution to $(\text{NLP-avg}(k, c, \epsilon))$ for $c = 2\pi$ and $c = \pi$, and for large enough k . In that direction, we refine the results reported in Theorem 8, and we solve $(\text{NLP-avg}(k, c, \epsilon))$ for $k = 2000$ inspection points to obtain slightly improved upper bounds, as shown in Table 3 on page 6.

In Figure 1 on page 7, we depict the derived trajectory for $\mathcal{P}(2\pi)$ and $\mathcal{P}(\pi)$, corresponding to solutions to \mathcal{S}_1 and \mathcal{S}_2 , respectively. In Figure 13, we show the corresponding values of t_i returned by $(\text{NLP-avg}(k, c, \epsilon))$ which are bounded away from 0. Finally, the values returned by the NLP for the angle θ for \mathcal{S}_1 and \mathcal{S}_2 were $\theta = 0.5910554, 0.8054878$, respectively (while for $n \geq 3$, we use $\theta = \pi/n$ as explained before). \square

5 Worst/Average Case Inspection Trade-offs to \mathcal{S}_1

The purpose of this section is twofold. First, we demonstrate that the upper bound we achieve for the average inspection cost of \mathcal{S}_1 using $\text{EPS}(\theta, t_1, \dots, t_k)$ represents a significant improvement over previously known trajectories. Second, we show that our techniques also address the multi-objective optimization problem of simultaneously minimizing the worst-case and average-case inspection times. This is achieved by considering the trade-off problem $\mathcal{T}(\lambda)$, leading to the proof of one of our main contributions, Theorem 4, which establishes Pareto upper bounds for the multi-objective inspection problem.

5.1 Pareto Upper Bounds

We begin by considering the *Isbell-type* family of trajectories for \mathcal{S}_1 , introduced in [46] as part of Theorem 1, parameterized by the deployment angle θ . Figure 5b shows this trajectory for $\mathcal{P}(c)$. This family of trajectories also appears in Theorem 5, where it establishes the optimal worst-case inspection solution for $\mathcal{P}(c)$ with $c \in [5\pi/6, 2\pi]$ (where $\mathcal{P}(2\pi)$ corresponds to \mathcal{S}_1).

In the *Isbell-type* trajectory with parameter $\theta \in [0, \pi/2)$, we define the point $A_0 = (1, \tan(\theta))$. The agent starts from the center of the disk and moves to A_0 (see Figure 5b on page 12 and Figure 12a on page 23). The agent then follows the tangent point $D' = \mathcal{P}_{2\theta}$ on the disk, searches the disk counterclockwise to point $D = \mathcal{P}_{3\pi/2}$, and finally moves along the projection to the tangent line at $\mathcal{P}_{2\pi}$, given by the line $x = 1$.

Lemma 6. *For every $\theta \in [0, \pi/2)$, the Isbell-type trajectory with deployment angle θ has the following inspection performance.*

- (a) *The worst case inspection equals $I_W(\theta) := 1/\cos(\theta) + \tan(\theta) + 3\pi/2 - 2\theta + 1$.*
- (b) *The average case inspection cost equals*

$$I_A(\theta) := \frac{1}{2\pi} \left(\log \left(\frac{1 + \sin(\theta)}{1 - \sin(\theta)} \right) + 2\theta^2 - 4\pi\theta + 2(\pi - \theta) \tan(\theta) + \frac{2(\pi - \theta)}{\cos(\theta)} + \frac{15\pi^2}{8} + \log 2 \right).$$

Proof. (a) In Theorem 2, we analyzed the performance of the generalized Isbell-type algorithm for solving $\mathcal{P}(c)$ for all $c \in [\pi/2, 2\pi]$. In our case, $c = 2\pi$ (corresponding to \mathcal{S}_1), resulting in the worst-case cost denoted as $f_2(\theta)$ in the proof of Theorem 2, which is the worst case inspection cost promised in the current lemma.

- (b) The points \mathcal{P}_ϕ , with $\phi \in [0, 2\pi]$, are inspected in 3 phases by the Isbell-type trajectory with parameter θ . First, the portion $O \rightarrow A_0$ of the trajectory inspects, by Lemma 1(b), all points with $\phi \in [0, 2\theta]$. The cumulative cost of the points inspected in this phase is, by Lemma 3(c) equal to $\log \left(\frac{1 + \sin(\theta)}{1 - \sin(\theta)} \right)$.

Then, the movement $A_0 \rightarrow D'$ inspects only the point $\mathcal{P}_{2\theta}$ already inspected in the previous phase. This is followed by the counter clockwise movement along the arc with endpoints $D' = \mathcal{P}_{2\theta}$ and $D = \mathcal{P}_{3\pi/2}$. For each $\phi \in [2\theta, 3\pi/2]$, we have $\mathcal{I}(\mathcal{P}_\phi) = OA_0 + A_0D' + \phi - 2\theta$, where $OA_0 = 1/\cos(\theta)$ as calculated in the proof of Lemma 3(b), and $A_0D = A_0\mathcal{P}_0 = \tan(\theta)$, by the definition of point A_0 (see also Figure 5b). We conclude that the cumulative inspection cost in this phase is

$$\begin{aligned} \int_{2\theta}^{3\pi/2} \mathcal{I}(\phi) d\phi &= \int_{2\theta}^{3\pi/2} \left(\frac{1}{\cos(\theta)} + \tan(\theta) + \phi - 2\theta \right) d\phi \\ &= \left(\frac{3\pi}{2} - 2\theta \right) \left(\frac{1}{\cos(\theta)} + \tan(\theta) - 2\theta \right) + \frac{9\pi^2}{8} - 2\theta^2 \end{aligned}$$

Finally, the trajectory concludes with movement $\mathcal{P}_{3\pi/2} \rightarrow F$, where F is the intersection of point of tangent lines $\mathcal{L}_{3\pi/2}$ and $\mathcal{L}_0 = \mathcal{L}_{2\pi}$, that is $F = (-1, 0)$, see Figure 10. This phase inspects \mathcal{P}_ϕ with $\phi \in [3\pi/2, 2\pi]$ and for each such point we find its inspection time $\mathcal{I}(\phi)$. Note that in order to reach point $\mathcal{P}_{3\pi/2}$, and by our previous analysis, time $1/\cos(\theta) +$

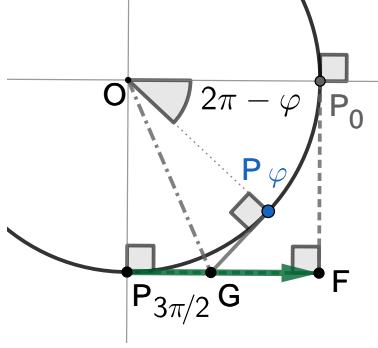


Fig. 10: The last phase of the Isbell-type algorithm for $\mathcal{P}(2\pi)$ (also \mathcal{S}_1).

$\tan(\theta) + 3\pi/2 - 2\theta$ has passed. The additional time that is needed to inspect \mathcal{P}_ϕ is by Lemma 1(c) equal to the length of $\mathcal{P}_{3\pi/2}G$. Now, the angle of triangle $GOP_{3\pi/2}$ (at vertex O) is $(\pi/2 - (2\pi - \phi))/2 = \phi/2 - 3\pi/4$, since triangles $GOP_{3\pi/2}, GOP_\phi$ are equal. But then $\mathcal{P}_{3\pi/2}G = \tan(\phi/2 - 3\pi/4)$, making the cumulative cost in this case equal to

$$\begin{aligned} \int_{3\pi/2}^{2\pi} \mathcal{I}(\phi) d\phi &= \frac{\pi}{2} \left(\frac{1}{\cos(\theta)} + \tan(\theta) + 3\pi/2 - 2\theta \right) + \int_{3\pi/2}^{2\pi} \tan(\phi/2 - 3\pi/4) d\phi \\ &= \frac{\pi}{2} \left(\frac{1}{\cos(\theta)} + \tan(\theta) + 3\pi/2 - 2\theta \right) + \log 2, \end{aligned}$$

where the last equality is based on that $\int \tan(x) = -\log(\cos(x))$. Adding then all cumulative inspection costs and scaling by 2π gives the average inspection cost, as described in the lemma. \square

The value of θ that minimizes the worst-case inspection cost $I_W(\theta)$, as described in Lemma 6, is $\theta_W = \pi/6 \approx 0.523599$ (see also Theorem 1 from [46], or our more general Theorem 2 for $n = 1$). For this value of θ_W , we have $I_W(\theta_W) = 1 + \sqrt{3} + \frac{7\pi}{6} \approx 6.39724$ and $I_A(\theta_W) = \frac{5}{2\sqrt{3}} + \frac{91\pi}{144} + \frac{\log(6)}{2\pi} \approx 3.71386$. Similarly, the value of θ that minimizes the average inspection cost $I_A(\theta)$, from Lemma 6, is $\theta_A = 0.592334$, which results in :

$$\begin{aligned} I_W(\theta_A) &\approx 6.406, \\ I_A(\theta_A) &\approx 3.70737. \end{aligned}$$

We expect the Pareto frontier of Isbell-type algorithms to be determined by $\theta \in [0.52359, 0.59233]$. However, for completeness, we plot the pairs $I(\theta) := (I_W(\theta), I_A(\theta))$ for all $\theta \in [0.4, 0.75]$ in Figure 2, on page 8.

In Theorem 3, we achieved an average inspection cost as low as 3.5509015. We are ready to demonstrate how to significantly improve both the worst-case and average inspection costs across the entire Pareto frontier, effectively proving Theorem 4.

Proof (of Theorem 4). The upper bound to the Pareto frontier will be obtained by the family of algorithms $\text{EPS}(\theta, t_1, \dots, t_k)$, with $k = 1000$, and for appropriate choices of parameters θ, t_i .

For this, we recall Lemma 3(b), from which for any feasible choice of the parameters, we obtain a formula $S_W(\theta, t_1, \dots, t_k)$ for the worst case cost. Let also $S_A(\theta, t_1, \dots, t_k)$ denote the objective of $(\text{NLP-avg}(k, c, \epsilon))$, with $c = 2\pi$ and $\epsilon = 10^{-3}$. For all NLP solutions we obtain, the optimizer values for θ are bounded away from $\pi/2$ (in fact, they admit values in $[0.5, 0.6]$), and hence the value of ϵ does not affect the cost of the solution, rather only is there to justify its correctness (see also Figure 11). According to Lemma 5, $S_A(\theta, t_1, \dots, t_k)$ correctly quantifies

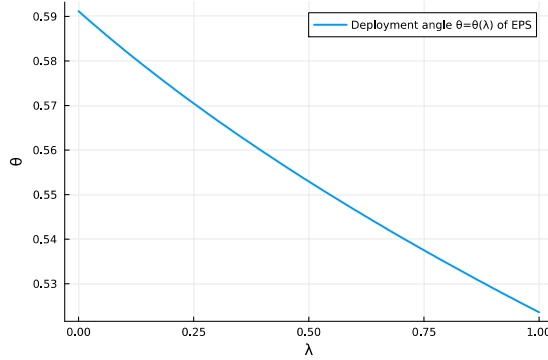


Fig. 11: The value of the initial deployment angle θ of trajectory $\text{EPS}(\theta, t_1, \dots, t_k)$ designed to minimize the trade-off problem $\mathcal{T}(\lambda)$, as a function of $\lambda \in [0, 1]$.

an upper bound to the average inspection cost to $\text{EPS}(\theta, t_1, \dots, t_k)$, for any feasible solution $(\theta, t_1, \dots, t_k)$ to the NLP.

Consequently, the new nonlinear program with objective

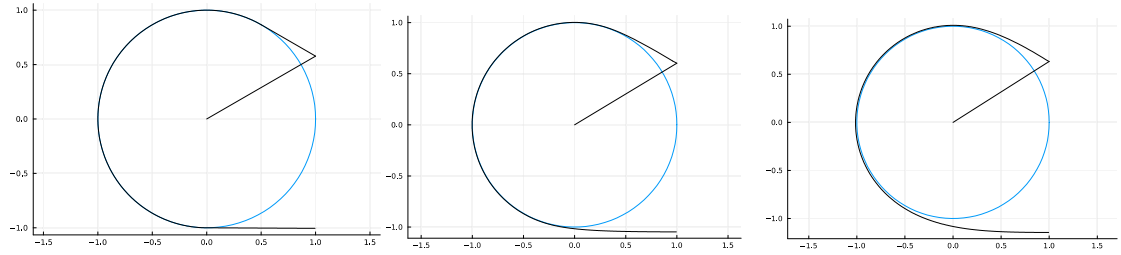
$$\lambda S_W(\theta, t_1, \dots, t_k) + (1 - \lambda) S_A(\theta, t_1, \dots, t_k)$$

and subject to the same constraints as in $(\text{NLP-avg}(k, c, \epsilon))$, correctly quantifies the objective for the trade-off problem $\mathcal{T}(\lambda)$.

For every λ from 0 to 1 and with step size 0.01, solving the new NLP we obtain a solution $(\theta(\lambda), t_1(\lambda), \dots, t_k(\lambda))$, and we define quantities $N_W(\lambda) := S_W(\theta(\lambda), t_1(\lambda), \dots, t_k(\lambda))$, and $N_A(\lambda) := S_A(\theta(\lambda), t_1(\lambda), \dots, t_k(\lambda))$. Thus, $N_W(\lambda)$ and $N_A(\lambda)$ accurately quantify the worst-case inspection cost and average inspection cost, respectively, for feasible $\text{EPS}(\theta(\lambda), t_1(\lambda), \dots, t_k(\lambda))$. As expected, $\lambda = 1$ provides an approximation of the worst-case optimal inspection trajectory and a precise quantification of its average inspection cost. Indeed, $N_W(1) \approx 6.3972578$ and $N_A(1) \approx 3.71130923$ (compare these to $I_W(\theta_W)$ and $I_A(\theta_W)$ respectively of the Isbell-type algorithm, and note that due to the feasibility lower bound on the t_i 's imposed in the NLP, the average inspection cost is slightly improved, whereas the worst case cost is slightly compromised). Similarly, the solution for $\lambda = 0$ yields the average inspection upper bound $N_A(0)$ from Theorem 3 for $\mathcal{P}(2\pi)$ (equivalently, \mathcal{S}_1) and a worst-case inspection cost of $N_W(0) = 6.8867382$. We conclude with Figure 2 on page 8, where we depict the pair $(N_W(\lambda), N_A(\lambda))$ for $\lambda \in [0, 1]$. \square

Trajectories that certify the reported average inspection cost upper bounds for $\mathcal{T}(\lambda)$ are depicted in Figure 12, with $\lambda = 1$ corresponding to optimizing the worst-case cost, and for

$\lambda = 2/3$ and $\lambda = 1/3$. Recall that the trajectory certifying the upper bound for $\mathcal{T}(0)$, which minimizes the average inspection cost, is shown in Figure 1a on page 7. The values of $t \in \mathbb{R}^k$ obtained as solutions to the nonlinear program described in the proof of Theorem 4 are shown in Figure 15 on page 30 for $\mathcal{T}(1)$, $\mathcal{T}(2/3)$, and $\mathcal{T}(1/3)$. Additionally, Figure 13b on page 29 presents the values of these parameters for $\mathcal{T}(0)$.



(a) The trajectory of the optimal $\text{EPS}(\theta, t_1, \dots, t_k)$ for solving $\mathcal{T}(1)$. The values of the corresponding values t_i are seen in Figure 15a.

(b) The trajectory of the optimal $\text{EPS}(\theta, t_1, \dots, t_k)$ for solving $\mathcal{T}(2/3)$. The values of the corresponding values t_i are seen in Figure 15b.

(c) The trajectory of the optimal $\text{EPS}(\theta, t_1, \dots, t_k)$ for solving $\mathcal{T}(1/3)$. The values of the corresponding values t_i are seen in Figure 15c.

Fig. 12: Agent's trajectories for trade-off problem $\mathcal{T}(\lambda)$ of the proof of Theorem 3, for $\lambda = 1, 2/3, 1/3$, using algorithm $\text{EPS}(\theta, t_1, \dots, t_k)$ with $k = 1000$. The trajectory corresponding to $\lambda = 0$ (i.e. the best average performance of $\text{EPS}(\theta, t_1, \dots, t_k)$ solving \mathcal{S}_1) can be seen in Figure 1a.

References

- [1] S. Acharjee, K. Georgiou, S. Kundu, and A. Srinivasan. Lower bounds for shoreline searching with 2 or more robots. In *23rd OPODIS*, volume 153 of *LIPICs*, pages 26:1–26:11. Schloss Dagstuhl - LZI, 2019.
- [2] R. Ahlswede and I. Wegener. *Search problems*. John Wiley & Sons, Inc., 1987.
- [3] S. Alpern, R. Fokkink, L. Gasieniec, R. Lindelauf, and V. S. Subrahmanian. *Search theory*. Springer, 2013.
- [4] S. Alpern and S. Gal. *The theory of search games and rendezvous*, volume 55. Springer Science & Business Media, 2006.
- [5] S. Angelopoulos, C. Dürr, and T. Lidbetter. The expanding search ratio of a graph. *Discret. Appl. Math*, 260:51–65, 2019.
- [6] R. Baeza-Yates. Searching: an algorithmic tour. *Encyclopedia of Computer Science and Technology*, 37:331–359, 1997.
- [7] R. Baeza-Yates and R. Schott. Parallel searching in the plane. *Computational Geometry*, 5(3):143–154, 1995.
- [8] R. A. Baeza-Yates, J. C. Culberson, and G. J. E. Rawlins. Searching with uncertainty. In *Scandinavian Workshop on Algorithm Theory*, pages 176–189. Springer, 1988.
- [9] R. A. Baeza-Yates, J. C. Culberson, and G. J. E. Rawlins. Searching in the plane. *Information and computation*, 106(2):234–252, 1993.
- [10] I. Bagheri, L. Narayanan, and J. Opatrny. Evacuation of equilateral triangles by mobile agents of limited communication range. In F. Dressler and C. Scheideler, editors, *ALGOSENSORS 2019*, volume 11931 of *Lecture Notes in Computer Science*, pages 3–22. Springer, 2019.
- [11] E. Bampas, J. Czyzowicz, L. Gasieniec, D. Ilcinkas, R. Klasing, T. Kociumaka, and D. Pajak. Linear search by a pair of distinct-speed robots. *Algorithmica*, 81(1):317–342, 2019.
- [12] A. Beck. On the linear search problem. *Israel Journal of Mathematics*, 2(4):221–228, 1964.
- [13] P. Behrouz, O. Konstantinidis, N. Leonardos, A. Pagourtzis, I. Papaioannou, and M. Spyraou. Byzantine fault-tolerant protocols for (n, f) -evacuation from a circle. In *International Symposium on Algorithmics of Wireless Networks*, pages 87–100. Springer, 2023.
- [14] R. Bellman. Minimization problem. *Bull. Amer. Math. Soc*, 62(3):270, 1956.
- [15] R. Bellman. Dynamic programming. *Chapter IX, Princeton University Press, Princeton, New Jersey*, 1958.
- [16] R. Bellman. An optimal search. *Siam Review*, 5(3):274, 1963.
- [17] G. Berzsenyi. Lost in a forest (a problem area initiated by the late richard e. bellman). *Quantum (November/December, 1995)*, 41, 1995.
- [18] A. Bonato, K. Georgiou, C. MacRury, and P. Prałat. Algorithms for p -faulty search on a half-line. *Algorithmica*, pages 1–30, 2022.
- [19] S. Bouchard, Y. Dieudonné, A. Pelc, and F. Petit. Deterministic treasure hunt in the plane with angular hints. In *29th International Symposium on Algorithms and Computation, ISAAC 2018*, volume 123, pages 48–1. Schloss Dagstuhl–Leibniz-Zentrum fuer Informatik, 2018.
- [20] S. Brandt, K.-T. Foerster, B. Richner, and R. Wattenhofer. Wireless evacuation on m rays with k searchers. *Theor. Comput. Sci*, 811:56–69, 2020.
- [21] M. Chrobak, L. Gasieniec, T. Gorry, and R. Martin. Group search on the line. In G. F. Italiano, T. Margaria-Steffen, J. Pokorný, J.-J. Quisquater, and R. Wattenhofer, editors,

- SOFSEM*, volume 8939 of *Lecture Notes in Computer Science*, pages 164–176. Springer, 2015.
- [22] H. Chuangpishit, K. Georgiou, and P. Sharma. A multi-objective optimization problem on evacuating 2 robots from the disk in the face-to-face model; trade-offs between worst-case and average-case analysis. *Information*, 11(11):506, 2020.
- [23] COIN-OR. Ipopt: Interior point optimizer. <https://github.com/coin-or/Ipopt>. Accessed: 2024-06-19.
- [24] J. Conley and K. Georgiou. Multi-agent disk inspection. In U. Schmid and R. Kuznets, editors, *SIROCCO 2025*, Lecture Notes in Computer Science. Springer, 2025.
- [25] J. Czyzowicz, L. Gasieniec, T. Gorry, E. Kranakis, R. Martin, and D. Pajak. Evacuating robots via unknown exit in a disk. In F. Kuhn, editor, *DISC 2014*, volume 8784 of *Lecture Notes in Computer Science*, pages 122–136. Springer, 2014.
- [26] J. Czyzowicz, K. Georgiou, M. Godon, E. Kranakis, D. Krizanc, W. Rytter, and M. Włodarczyk. Evacuation from a disc in the presence of a faulty robot. In S. Das and S. Tixeuil, editors, *SIROCCO 2017*, volume 10641 of *Lecture Notes in Computer Science*, pages 158–173. Springer, 2017.
- [27] J. Czyzowicz, K. Georgiou, and E. Kranakis. Group search and evacuation. In P. Flocchini, G. Prencipe, and N. Santoro, editors, *Distributed Computing by Mobile Entities; Current Research in Moving and Computing*, chapter 14, pages 335–370. Springer, 2019.
- [28] J. Czyzowicz, E. Kranakis, D. Krizanc, L. Narayanan, J. Opatrny, and S. M. Shende. Wireless autonomous robot evacuation from equilateral triangles and squares. In S. Papavassiliou and S. Ruehrup, editors, *14th International Conference, ADHOC-NOW*, volume 9143 of *Lecture Notes in Computer Science*, pages 181–194. Springer, 2015.
- [29] J. Czyzowicz, E. Kranakis, D. Krizanc, L. Narayanan, J. Opatrny, and S. M. Shende. Linear search with terrain-dependent speeds. In D. Fotakis, A. Pagourtzis, and V. Th. Paschos, editors, *Algorithms and Complexity - 10th International Conference, CIAC 2017, Athens, Greece, May 24-26, 2017, Proceedings*, volume 10236 of *Lecture Notes in Computer Science*, pages 430–441, 2017.
- [30] S. Dobrev, R. Kráľovič, and D. Pardubská. Improved lower bounds for shoreline search. In *International Colloquium on Structural Information and Communication Complexity*, pages 80–90. Springer, 2020.
- [31] I. Dunning, J. Huchette, and M. Lubin. Jump: A modeling language for mathematical optimization. *SIAM review*, 59(2):295–320, 2017.
- [32] Y. Emek, T. Langner, D. Stolz, J. Uitto, and R. Wattenhofer. How many ants does it take to find the food? *Theoretical Computer Science*, 608:255–267, 2015.
- [33] Y. Emek, T. Langner, J. Uitto, and R. Wattenhofer. Solving the ants problem with asynchronous finite state machines. In *Proceedings of International Colloquium on Automata, Languages, and Programming (ICALP), LNCS 8573*, pages 471–482, 2014.
- [34] S. P. Fekete, C. Gray, and A. Kröller. Evacuation of rectilinear polygons. In W. Wu and O. Daescu, editors, *Combinatorial Optimization and Applications - 4th International Conference, COCOA 2010, Kailua-Kona, HI, USA, December 18-20, 2010, Proceedings, Part I*, volume 6508 of *Lecture Notes in Computer Science*, pages 21–30. Springer, 2010.
- [35] S. R. Finch and J. E. Wetzel. Lost in a forest. *The American Mathematical Monthly*, 111(8):645–654, 2004.
- [36] S. R. Finch and L.-Y. Zhu. Searching for a shoreline. *arXiv preprint math/0501123*, 2005.
- [37] G. M. Fricke, J. P. Hecker, A. D. Griego, L. T. Tran, and M. E. Moses. A distributed deterministic spiral search algorithm for swarms. In *2016 IEEE/RSJ International Conference on Intelligent Robots and Systems (IROS)*, pages 4430–4436. IEEE, 2016.
- [38] S. Gal. Search games. *Wiley Encyclopedia of Operations Research and Management Science*, 2010.

- [39] K. Georgiou and W. Jang. Triangle evacuation of 2 agents in the wireless model. In *Algorithmics of Wireless Networks: 18th International Symposium on Algorithmics of Wireless Networks, ALGOSENSORS 2022, Potsdam, Germany, September 8–9, 2022, Proceedings*, pages 77–90. Springer, 2022.
- [40] K. Georgiou, C. Jones, and J. Lucier. Multi-agent search-type problems on polygons. In *International Conference on Current Trends in Theory and Practice of Computer Science*, pages 314–332. Springer, 2025.
- [41] K. Georgiou, S. Leizerovich, J. Lucier, and S. Kundu. Evacuating from ℓ_p unit disks in the wireless model. *Theoretical Computer Science*, 944:113675, 2023.
- [42] K. Georgiou and J. Lucier. Weighted group search on a line & implications to the priority evacuation problem. *Theoretical Computer Science*, 939:1–17, 2023.
- [43] P. Gibbs. Bellman’s escape problem for convex polygons, 2016.
- [44] B. Gluss. An alternative solution to the “lost at sea” problem. *Naval Research Logistics Quarterly*, 8(1):117–122, 1961.
- [45] B. Gluss. The minimax path in a search for a circle in a plane. *Naval Research Logistics Quarterly*, 8(4):357–360, 1961.
- [46] J. R. Isbell. An optimal search pattern. *Naval Research Logistics Quarterly*, 4(4):357–359, 1957.
- [47] A. Jeż and J. Łopuszański. On the two-dimensional cow search problem. *Information Processing Letters*, 109(11):543–547, 2009.
- [48] J. M. Kleinberg. On-line search in a simple polygon. In *SODA*, volume 94, pages 8–15. Citeseer, 1994.
- [49] D. Kübel and E. Langetepe. On the approximation of shortest escape paths. *Computational Geometry*, 93:101709, 2021.
- [50] E. Langetepe. On the optimality of spiral search. In *Proceedings of the twenty-first annual ACM-SIAM symposium on Discrete Algorithms*, pages 1–12. SIAM, 2010.
- [51] E. Langetepe. Searching for an axis-parallel shoreline. *Theoretical Computer Science*, 447:85–99, 2012.
- [52] T. Langner, B. Keller, J. Uitto, and R. Wattenhofer. Overcoming obstacles with ants. In E. Anceaume, C. Cachin, and M. G. Potop-Butucaru, editors, *International Conference on Principles of Distributed Systems (OPODIS)*, volume 46 of *LIPICs*, pages 9:1–9:17. Schloss Dagstuhl - Leibniz-Zentrum fuer Informatik, 2015.
- [53] D. Pattanayak, H. Ramesh, P. S. Mandal, and S. Schmid. Evacuating two robots from two unknown exits on the perimeter of a disk with wireless communication. In *Proceedings of the 19th International Conference on Distributed Computing and Networking*, pages 1–4, 2018.
- [54] A. Pelc. Reaching a target in the plane with no information. *Information Processing Letters*, 140:13–17, 2018.
- [55] A. Pelc and R. N. Yadav. Information complexity of treasure hunt in geometric terrains. *arXiv preprint arXiv:1811.06823*, 2018.
- [56] A. Pelc and R. N. Yadav. Cost vs. information tradeoffs for treasure hunt in the plane. *arXiv preprint arXiv:1902.06090*, 2019.
- [57] D. O. Shklarsky, N. N. Chentzov, and I. M. Yaglom. *The USSR Olympiad Problem Book: Selected Problems and Theorems of Elementary Mathematics, Part 2, Volume II*. Nauka Publishers, Moscow, 1962.

A Omitted Proofs

A.1 Proofs Omitted from Section 3.2

Lemma 7. For every $c \in [0, 3\pi/2]$, function $f_1(\theta) := 1/\cos(\theta) + \sin(c - \theta - \pi/2)/\cos(\theta) + 1$, subject to that $\theta \geq c/2 - \pi/4$ and $\theta < \pi/2$, attains the following minima:

$$\begin{cases} f_1(c/2), & \text{if } 0 \leq c \leq 2\pi/3 \\ f_1(\pi - c), & \text{if } 2\pi/3 < c \leq 5\pi/6 \\ f_1(c/2 - \pi/4), & \text{if } 5\pi/6 < c \leq 3\pi/2. \end{cases}$$

Proof. For every $c \in [0, 3\pi/2]$, we aim to find the minimum of the function $f_1(\theta) = \frac{1 + \sin(c - \theta - \pi/2)}{\cos \theta} + 1$, subject to the constraints $\theta \geq \frac{c}{2} - \frac{\pi}{4}$ and $\theta < \frac{\pi}{2}$. For this we rely on the derivative $f_1'(\theta) = (\sin(\theta) - \sin(c - \theta - \pi/2))/\cos(\theta)$. Next we examine cases for the range of parameter c .

Case 1: If $0 \leq c \leq \pi/2$, we have that that $f_1'(\theta) = 0$ if and only if $\theta = c$ (for $0 \leq \theta < \pi/2$), whereas $f_1'(0) = -\sin(c) < 0$. This means that the function is initially decreasing, up to $\theta = c$. However, $c/2 - \pi/4 \leq \theta \leq c/2 \leq c$, and therefore $f_1(\theta)$ is minimized at the end of its domain, that is at $\theta = c/2$,

Case 2: If $\pi/2 \leq c \leq \pi$, and since $0 \leq \theta < \pi/2$, we have that that $f_1'(\theta) = 0$ if and only if $\theta = \pi - c$. At the same time, $c/2 - \pi/4 \leq \theta \leq c/2$, hence we see that $c/2 - \pi/4 \leq \pi - c \leq c/2$ if and only if $2\pi/3 \leq c \leq 5\pi/6$. At the same time, for every $\epsilon > 0$ sufficiently small, we have that $f_1'(\pi - c - \epsilon) = (\sin(c + \epsilon) - \sin(c))/\cos(c + \epsilon)$ implying that f_1 is decreasing for $c \leq \pi - c$. We conclude that for $c \in [2\pi/3 \leq c \leq 5\pi/6]$, $f_1(\theta)$ is minimized at $\theta = \pi - c$. For $c \in [\pi/2, 2\pi/3]$, we have that $\pi - c \geq c/2$. Hence, $f_1(\theta)$, is decreasing up to $\theta \leq c/2$, and hence the minimum in this case is attained at $\theta = c/2$. Finally, for the case 2, if $c \in [5\pi/6, \pi]$, we have that $\pi - c \leq c/2 - \pi/4$, hence $f_1(\theta)$ is increasing when $\theta \in [c/2 - \pi/4, c/2]$, inducing the minimizer $\theta = c/2 - \pi/4$.

Case 3: Finally, if $\pi \leq c \leq 3\pi/2$, we have that $\sin(c) \leq 0$, and hence $f_1'(\theta) = (\sin(\theta) - \sin(c - \theta - \pi/2))/\cos(\theta) \geq 0$. For this reason, $f_1(\theta)$ is increasing in $[c/2 - \pi/4, \pi/2)$, and so the minimum is attained at $\theta = c/2 - \pi/4$. \square

Lemma 8. For every $c \in [\pi/2, 2\pi]$, function $f_2(\theta) = 1/\cos(\theta) + \tan(\theta) + c - \pi/2 - 2\theta + 1$, subject to that $0 \leq \theta \leq c/2 - \pi/4$ and $\theta < \pi/2$, attains the following minima:

$$\begin{cases} f_2(c/2 - \pi/4), & \text{if } \pi/2 \leq c \leq 5\pi/6 \\ f_2(\pi/6), & \text{if } 5\pi/6 < c \leq 2\pi. \end{cases}$$

Proof. For each fixed parameter $c \in [\pi/2, 2\pi]$, we study the monotonicity of $f_2(\theta) = 1/\cos(\theta) + \tan(\theta) + c - \pi/2 - 2\theta + 1$ in the domain identified by that $0 \leq \theta \leq c/2 - \pi/4$ and $\theta < \pi/2$. For this we see that $f_2'(\theta) = (1/\cos(\theta) + \tan(\theta))/\cos(\theta) - 2$, and that $f_2''(\theta) = (1/\cos(\theta) + \tan(\theta))^2/\cos(\theta)$.

The above imply that $f_2(\theta)$ is convex, and $f_2'(\theta)$ is increasing in $[0, \pi/2)$. The only root of $f_2'(\theta)$ in $[0, \pi/2)$ is at $\theta = \pi/6$, while it is also easy to see that $f_2'(0) = -1$. Therefore, $f_2(\theta)$ is initially decreasing, it is minimized at $\theta = \pi/6$, and then it is increasing for up to $\theta < \pi/2$.

We recall the domain of $f_2(\theta)$, identified by that $0 \leq \theta \leq c/2 - \pi/4$ and $\theta < \pi/2$. Hence, $\theta = \pi/6$ is a minimizer if and only if $\pi/6 \leq c/2 - \pi/4$ iff and only if $c \in [5\pi/6, 2\pi]$. For parameters $c \in [\pi/2, 5\pi/6]$, we see that $f_2(\theta)$ is decreasing in its domain, and hence it is minimized at $\theta = c/2 - \pi/4$. \square

Lemma 9. For every $c \in [\pi/2, 3\pi/2]$, let $f_1(\theta), f_2(\theta)$ be as in Lemma 7 and Lemma 8. Let θ_1, θ_2 denote the corresponding minimizers. Then,

$$\min\{f_1(\theta_1), f_2(\theta_2)\} = \begin{cases} f_1(c/2) = 1/\cos(c/2) & \text{if } \pi/2 \leq c \leq 2\pi/3 \\ f_1(\pi - c) = 1 - 2\cos(c) & \text{if } 2\pi/3 < c \leq 5\pi/6 \\ f_2(\pi/6) = \sqrt{3} + c - 5\pi/6 + 1 & \text{if } 5\pi/6 < c \leq 2\pi \end{cases}$$

Proof. For each $c \in [0, 2\pi]$, let $\theta_1 = \theta_1(c), \theta_2 = \theta_2(c)$ denote the minimizers of $f_1(\theta), f_2(\theta)$ as in Lemma 7 and Lemma 8, and for the values of c that each is defined. By direct substitution we see that

$$f_1(\theta_1) = \begin{cases} 1/\cos(c/2), & \text{if } 0 \leq c \leq 2\pi/3 \\ 1 - 2\cos(c), & \text{if } 2\pi/3 < c \leq 5\pi/6 \\ 1 + 1/\sin(c/2 + \pi/4) + \tan(c/2 - \pi/4), & \text{if } 5\pi/6 < c \leq 3\pi/2. \end{cases}$$

and

$$f_2(\theta_2) = \begin{cases} 1 + 1/\sin(c/2 + \pi/4) + \tan(c/2 - \pi/4), & \text{if } \pi/2 \leq c \leq 5\pi/6 \\ \sqrt{3} + c - 5\pi/6 + 1, & \text{if } 5\pi/6 < c \leq 2\pi. \end{cases}$$

For $c \leq \pi/2$ only $f_1(\theta_1)$ is defined, while for $c \geq 3\pi/2$ only $f_2(\theta_2)$ is defined. Taking also the piece-wise definition of the minimizers, we conclude that $\min\{f_1(\theta_1), f_2(\theta_2)\}$ over $c \in [\pi/2, 3\pi/2]$ should be analyzed in the following three subintervals.

$$\begin{aligned} M_1 &:= \min_{c \in [\pi/2, 2\pi/3]} \{f_1(\theta_1), f_2(\theta_2)\} = \min \left\{ \frac{1}{\cos(c/2)}, 1 + \frac{1}{\sin(c/2 + \pi/4)} + \tan(c/2 - \pi/4) \right\} \\ M_2 &:= \min_{c \in [2\pi/3, 5\pi/6]} \{f_1(\theta_1), f_2(\theta_2)\} = 1 + \min \left\{ -2\cos(c), \frac{1}{\sin(c/2 + \pi/4)} + \tan(c/2 - \pi/4) \right\} \\ M_3 &:= \min_{c \in [5\pi/6, 3\pi/2]} \{f_1(\theta_1), f_2(\theta_2)\} = 1 + \min \left\{ \frac{1}{\sin(c/2 + \pi/4)} + \tan(c/2 - \pi/4), \sqrt{3} + c - 5\pi/6 \right\} \end{aligned}$$

We claim that $M_1 = \cos(c/2)$, and for this we consider function

$$g_1(c) = \frac{1}{\sin(c/2 + \pi/4)} + \tan(c/2 - \pi/4) + 1 - \frac{1}{\cos(c/2)}$$

over $c \in [\pi/2, 2\pi/3]$. We will show that $g_1(c) \geq 0$. For this we see that $g_1(2\pi/3) = (\sqrt{2} - 1)(\sqrt{3} - 1) > 0$. Hence, it suffices to show that $g_1(c)$ is decreasing. First it is easy to see that

$$g_1'(c) = \frac{1}{16} \sec^2\left(\frac{c}{2}\right) \sec^2\left(\frac{1}{8}(2c + \pi)\right) \left(-4 \sin\left(\frac{c}{2}\right) - 2 \sin\left(c + \frac{\pi}{4}\right) + 2 \cos(c) + \sqrt{2} + 2\right).$$

Hence, it suffices to show that $h_1(c) = -4 \sin\left(\frac{c}{2}\right) - 2 \sin\left(c + \frac{\pi}{4}\right) + 2 \cos(c) + \sqrt{2} + 2 < 0$ for $c \in [\pi/2, 2\pi/3]$. Indeed, we have $h_1(c) = 2 - 2\sqrt{2} < 0$. Hence, it further suffices to show that $h_1(c)$ is decreasing. To that end we note that $\sin(c)$ is strictly decreasing in $c \in [\pi/2, 2\pi/3]$, and hence, after performing the transformation $\sin(c) = x$, we obtain function

$$s_1(x) = h_1(\arcsin(x)) = -\sqrt{2 - 2x^2} - (\sqrt{2} - 2)x - 2\sqrt{2 - 2x} + \sqrt{2} + 2,$$

over the domain $x \in [\sqrt{3}/2, 1]$, which we need to show is increasing. For that, we calculate $s_1'(x) = \frac{2x}{\sqrt{2-2x^2}} + \frac{2}{\sqrt{2-2x}} - \sqrt{2} + 2$, which is well defined for all $x \in [\sqrt{3}/2, 1)$. But then, note that for all $x \geq 0$, we have that $s_1'(x) > 0$, hence indeed, $s_1(x)$ is increasing as wanted.

Next we claim that $M_2 = 1 - 2 \cos(c)$, and for this we consider function

$$g_2(c) = \frac{1}{\sin(c/2 + \pi/4)} + \tan(c/2 - \pi/4) + 2 \cos(c)$$

over $c \in [2\pi/3, 5\pi/6]$. We see that $g_2(5\pi/6) = 0$, and hence it is enough to show that $g_2(c) \geq 0$. For this we calculate $g_2'(c) = \frac{1}{4} \sec^2(\frac{1}{8}(2c + \pi)) - 2 \sin(c)$, and we show that $g_2'(c) \leq 0$, for all $c \in [2\pi/3, 5\pi/6]$, implying that $g_2(c)$ is decreasing, and hence concluding what we claimed. To show that the derivative is negative, we apply transformation $x = \cos(c/4 + \pi/8)$, hence defining function

$$s_2(x) = g_2(4 \arccos(x) - \pi/2) = 2 + 1/(4x^2) - 16x^2 + 16x^4$$

with $1/2 \leq x \leq \sin(5\pi/24) \approx 0.608761$. Clearly, it suffices to show that $s_2(x) \leq 0$ in the latter interval. Applying also the transformation $2x^2 = y$, we obtain $s_2(\sqrt{y/2}) = 4y^2 - 8y + \frac{1}{2y} + 2 = \frac{8y^3 - 16y^2 + 4y + 1}{2y}$, and hence it suffices to prove that $q_2(y) = 8y^3 - 16y^2 + 4y + 1 \leq 0$, in the domain $1/2 \leq y \leq 2 \sin^2(\frac{5\pi}{24}) \approx 0.741181$ obtained from the transformation. The three real roots of $q_2(y)$ are easy to derive: $y_1 = 1/2, y_2 = \frac{1}{4}(3 - \sqrt{13}) \approx -0.151388$ and $y_3 = \frac{1}{4}(\sqrt{13} + 3) \approx 1.65139$. Since the leading coefficient of $q_2(y)$ is positive, it follows that $q_2(x)$ is negative for all $1/2 \leq y \leq \frac{1}{4}(\sqrt{13} + 3)$. The main claim then follows by noticing that $2 \sin^2(\frac{5\pi}{24}) \leq \frac{1}{4}(\sqrt{13} + 3)$.

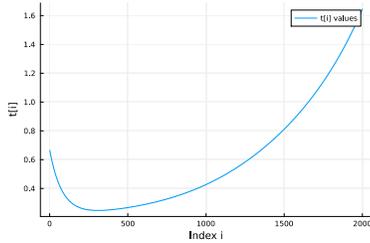
Finally, we claim that $M_3 = 1 + \sqrt{3} + c - 5\pi/6$, and for this we consider function

$$g_3(c) = \frac{1}{\sin(c/2 + \pi/4)} + \tan(c/2 - \pi/4) - \sqrt{3} - c + 5\pi/6$$

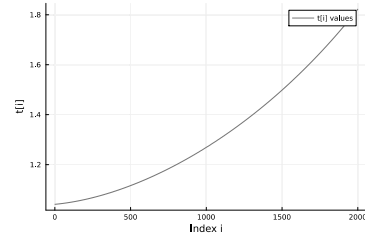
over $c \in [5\pi/6, 3\pi/2]$. We need to show that $g_3(c) \geq 0$, and we see that $g_3(5\pi/6) = 0$. Therefore, it suffices to prove that $g_3'(c) = -1 + 1/2 \cos^2(c/4 + \pi/8) \geq 0$. Recall that $c \in [5\pi/6, 3\pi/2]$, and hence $c/4 + \pi/8 \in [\pi/3, \pi/2]$. But then, since $\cos(\cdot)$ is decreasing in $[\pi/3, \pi/2]$, we see that $\cos(c/4 + \pi/8) \leq \cos(\pi/3) = 1/2$. This implies that $g_3'(c) = -1 + 1/4 \cos^2(c/4 + \pi/8) \geq -1 + 1/4 = -3/4 < 0$ as wanted. \square

B Omitted Figures

B.1 Figures Omitted from Section 4.2

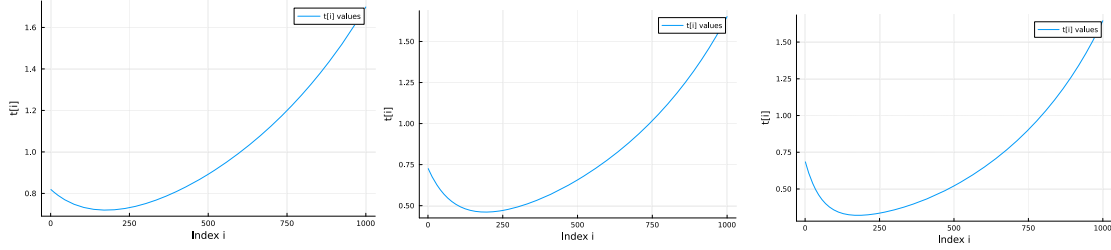


(a) The values of t_i for inspection trajectory $\text{EPS}(0.5910554, t_1, \dots, t_k)$, with $k = 2000$, for $\mathcal{P}(2\pi)$ as well as for \mathcal{S}_1 .



(b) The values of t_i for inspection trajectory $\text{EPS}(0.8054878, t_1, \dots, t_k)$, with $k = 2000$, for $\mathcal{P}(\pi)$ as well as for \mathcal{S}_2 .

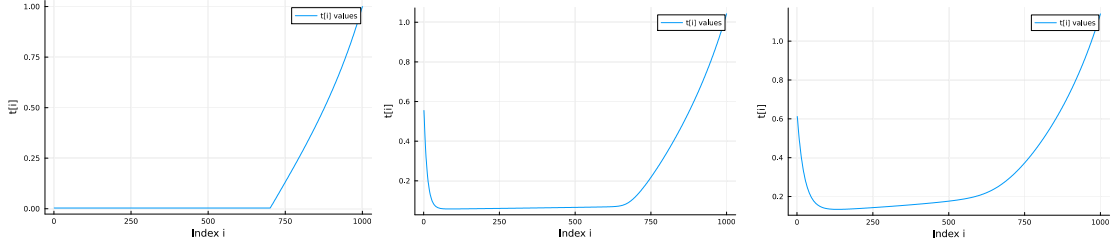
Fig. 13: Inspection parameter values of t_i for the extended polysegment algorithm, as used in Theorem 3.



(a) The values of t_i of trajectory $\text{EPS}(\theta, t_1, \dots, t_k)$ solving $\mathcal{P}(5\pi/4)$. The corresponding trajectory is seen in Figure 9a. (b) The values of t_i of trajectory $\text{EPS}(\theta, t_1, \dots, t_k)$ solving $\mathcal{P}(6\pi/4)$. The corresponding trajectory is seen in Figure 9c. (c) The values of t_i of trajectory $\text{EPS}(\theta, t_1, \dots, t_k)$ solving $\mathcal{P}(7\pi/4)$. The corresponding trajectory is seen in Figure 9c.

Fig. 14: Trajectories for minimizing the average inspection cost for $\mathcal{P}(c)$, $c = i\frac{\pi}{4}$, where $i = 5, 6, 7$.

B.2 Figures Omitted from Section 5



(a) The values of t_i of trajectory $\text{EPS}(\theta, t_1, \dots, t_k)$ solving $\mathcal{T}(1)$. The corresponding trajectory is seen in Figure 12a. (b) The values of t_i of trajectory $\text{EPS}(\theta, t_1, \dots, t_k)$ solving $\mathcal{T}(2/3)$. The corresponding trajectory is seen in Figure 12b. (c) The values of t_i of trajectory $\text{EPS}(\theta, t_1, \dots, t_k)$ solving $\mathcal{T}(1/3)$. The corresponding trajectory is seen in Figure 12c.

Fig. 15: Agent’s trajectories’ parameter values t_i for trade-off problem $\mathcal{T}(\lambda)$ of the proof of Theorem 3, for $\lambda = 1, 2/3, 1/3$. The parameter values corresponding to $\lambda = 0$ (i.e. the best average performance of $\text{EPS}(\theta, t_1, \dots, t_k)$ solving \mathcal{S}_1) can be seen in Figure 13b. Notably, for $\lambda = 1$, parameter values are nearly 0, satisfying constraint $t_i \geq (1 - \cos(\frac{c-2\theta}{k}))/\sin(\frac{c-2\theta}{k})$ tightly. For $\lambda = 2/3$ the values are bounded away from the threshold. For $\lambda = 1/3$, both the behavior of parameters t_i as well as the trajectory resemble those corresponding to $\lambda = 1$.